12-2008

Digital integration for monitoring acceleration signals

Charles Matthew Rose
University of Tennessee

To the Graduate Council:

I am submitting herewith a thesis written by Charles Matthew Rose entitled "Digital integration for monitoring acceleration signals." I have examined the final electronic copy of this thesis for form and content and recommend that it be accepted in partial fulfillment of the requirements for the degree of Master of Science, with a major in Electrical Engineering.

L. Montgomery Smith, Major Professor

We have read this thesis and recommend its acceptance:

Accepted for the Council:
Carolyn R. Hodges

Vice Provost and Dean of the Graduate School

(Original signatures are on file with official student records.)

To the Graduate Council:

I am submitting herewith a thesis written by Charles Matthew Rose entitled "Digital Integration for Monitoring Acceleration Signals." I have examined the final electronic copy of this thesis for form and content and recommend that it be accepted in partial fulfillment of the requirements for the degree of Master of Science, with a major in Electrical Engineering.

L. Montgomery Smith, Major Professor

We have read this thesis
and recommend its acceptance:

Bruce W. Bomar

Bruce A. Whitehead

Accepted for the Council:

Carolyn R. Hodges
Vice Provost and Dean of the Graduate School

(Original signatures are on file with official student records.)

Digital Integration for Monitoring Acceleration Signals

A Thesis

Presented for the

Master of Science

Degree

The University of Tennessee, Knoxville

Charles Matthew Rose

December 2008

ACKNOWLEDGEMENTS

The author wishes to thank Dr. Montgomery L. Smith for his advice and assistance in the preparation of this thesis. Appreciation is also expressed to The University of Tennessee Space Institute, Arnold Engineering Development Center (AEDC), the United States Air Force (USAF), and Aerospace Testing Alliance (ATA) for the opportunity to pursue this degree and complete this thesis.

The author also wishes to thank Mr. Philip Voyles and Mr. Brandon Jones for their advice and assistance on this study.

The research and results reported herein was performed by personnel of Aerospace Testing Alliance, support contractor for AEDC. Approved for Public Release; Distribution is unlimited. Further reproduction is authorized to satisfy the needs of the U.S. Government.

ABSTRACT

When testing turbine engines at Arnold Engineering Development Center (AEDC), vibration measurements are some of the most critical data taken. The present vibration monitoring system (VMS) consists of a charge producing accelerometer sensor, a charge amplifier, and a recording and analysis system. Currently the charge amplifier and the recording and analysis system are located in a data conditioning room which is approximately 150 feet from the accelerometer. If the signal processing equipment were moved closer to the test cell near the accelerometer, the fidelity of the acquired data could be greatly improved. An ideal system for this purpose would acquire acceleration data, digitize it, and send a digital data stream to a recording and analysis system outside the test cell. This type of system would minimize noise pickup and eliminate much of the hardware used in the current analog system. The digitizing hardware needed for a new system currently is available but a digital integrating filter is needed to produce velocity and displacement data. This thesis will study 8 candidate digital integrator designs to replace the analog integrator. These digital integrators will be compared to the ideal integrator by their mean square error. Actual accelerometer test data have been processed with the candidate digital filters for comparison to the mathematically correct solution of the integral. The thesis also describes the development of a digital filter to remove all DC offset for stability purposes. The combined digital filters will allow for the completion of the digital VMS and represent a significant increase in accuracy over the analog charge amplifier.

Table of Contents

List of Figures

List of Tables

Chapter 1

Introduction

Arnold Engineering Development Center (AEDC) contains a wide array of testing facilities, 14 of which are unique to the world. AEDC is a test center for the Department of Defense and is an Air Force Materiel Command Organization. The Air Force requires all top priority military aircraft under development to be tested at this facility in some capacity.

Testing at AEDC is generally classified under three categories: aerodynamic, aeropropulsion, and space and missiles. Aerodynamic testing usually includes a model of the actual aircraft that is scaled down to fit inside a transonic or supersonic wind tunnel. The models are tested at different altitudes to determine performance. The aeropropulsion group tests the turbine engines that are installed in the actual aircraft to verify their performance under varied altitude conditions inside test cells. Finally, the space and missiles test facilities deal with the performance of complete rocket systems and can also simulate space conditions in vacuum chambers.

In aeropropulsion tests, vibration measurements are some of the most important and closely scrutinized measurements taken. The data acquired is used to measure the engine's overall physical condition and health. If the vibration readings are unusual or high then it could indicate that some part of the engine is breaking apart. For this reason the vibration measurements are tied to an abort system where the engine will shut down after the vibration reaches a certain limit that has been established by the engine manufacturer.

The present Vibration Measurement System (VMS) consists of a piezoelectric accelerometer sensor that produces a current with a charge proportional to the acceleration of the component under test, an integrating analog charge amplifier with a built in charge-to-voltage converter, and a recording and analysis system. The accelerometer is typically located in the test cell on the test article. A microdot cable is used to connect the transducer to a permanent cell interface which usually consists of a bulkhead BNC connector and RG-58 cable that connects the sensor to the charge amplifier some distance away. Velocity and displacement are found by integrating the input acceleration signal. The integrated outputs from the charge amplifier are then connected to an analog-to-digital converter. The digitized data are then transferred to a data and analysis system called the Computer Aided Dynamic Data Analysis and Measurement System (CADDMAS). CADDMAS is a processing unit capable of hosting several display units for real time analysis and is also used to store data points for later study. The present VMS system is displayed in figure 1-1.

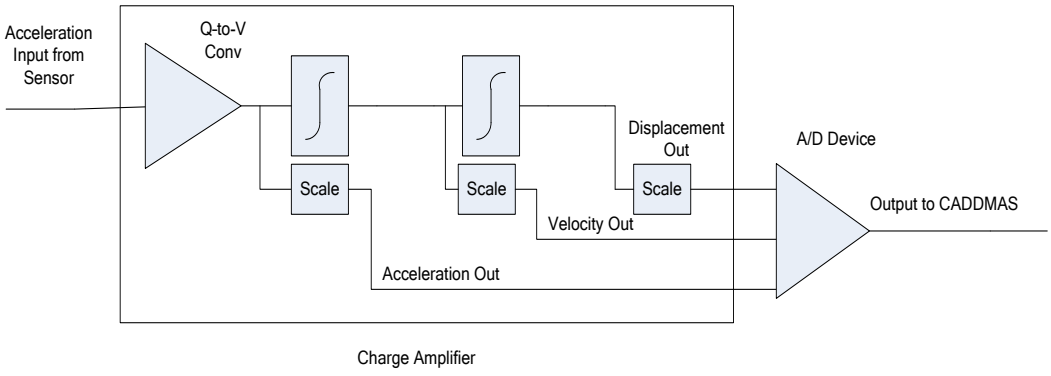

Figure 1-1: Current VMS Setup

In an effort to minimize noise and improve data signal fidelity, it would be advantageous to move as much of the acquisition and processing equipment as close to the source of the data as possible. While there are charge-to-voltage converters available that will convert the charge signal from the sensor to a voltage signal that is linearly proportional to the acceleration, a filter is required that would integrate the acceleration signal, after it has been digitized, into mathematically correct velocity and displacement signals. The ideal system would be one that acquires acceleration data, digitizes it, integrates it digitally to produce velocity and displacement data and sends a digital data stream to the CADDMAS. An ideal system is shown in figure 1-2.

This paper deals with the research, design, and comparison of such a digital integrator. The goal of the effort is to provide mathematically accurate velocity and displacement data. A total of 8 different digital integrators were investigated. The output of each digital integrator was compared to the mathematically correct solution and the output of the analog integration circuit inside the charge amplifier. It was found that by integrating in the time domain and then taking the FFT a more accurate answer could be produced than both previous attempts at a digital system and the current analog system.

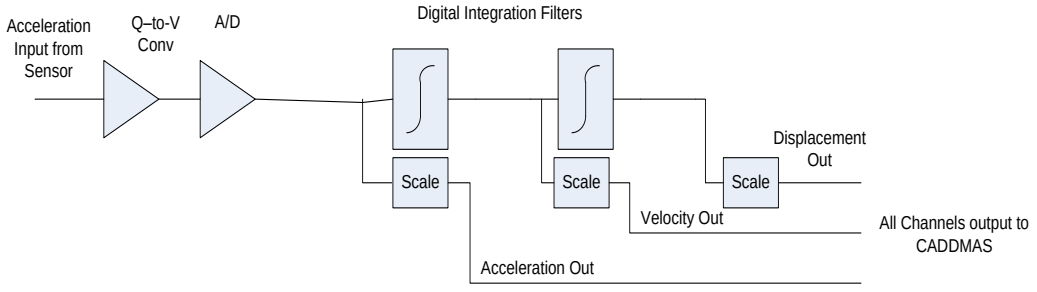

Figure 1-2: Ideal Digital VMS

Digital integration is an important concept in many engineering applications such as radar and control. Most of these applications that use digital integration are single tone signals. The integrator used for the digital VMS will need the ability to integrate a multi-tone signal correctly. Some basic integrators such as the rectangle, trapezoidal, and Simpson's methods are commonly used for these purposes. While these integrators are capable in many instances, this paper will strive to improve upon these commonly used integration methods by optimizing certain values or combining the digital filters with other techniques that will result in improved accuracy and repeatability.

Chapter 2 will depict the analog charge amplifier and describe its shortcomings in detail. Chapter 3 will describe the design of the proposed digital integrators. Chapter 4 will display results from the digital integrators with actual data acquired from an engine test. Finally, Chapter 5 will outline the recommended digital integrator for use in a digital VMS.

Chapter 2

Background

2.1 – Analog VMS

The current VMS in use at AEDC uses a charge amplifier with an analog integrator to produce velocity and displacement data. The individual analog signals are then input into the recording and analysis system where they are converted to a digital format.

The VMS uses piezoelectric accelerometers that are mounted on the test article in the test cell. A crystal lattice inside the accelerometer vibrates as the test article accelerates and converts the mechanical energy into electrical energy. The accelerometer outputs a linear charge, measured in picocoulombs, that is proportional to the acceleration seen by the crystal. This charge is carried by a current that is passed from a microdot cable attached to the accelerometer to a coaxial cable that carries it to a charge amplifier.

The charge amplifier is a special type of pre-amplifier that is used for piezoelectric accelerometers. As its name implies, the charge amplifier is sensitive to the amount of charge produced by the accelerometer rather than the voltage or current. Once it has received the charge input from the accelerometer, the charge amplifier integrates the signal to velocity and displacement then outputs a linear voltage for all three signals. The outputs are all scaled for units of G's for acceleration, inches per second for velocity, and mills for displacement. The charge amplifier provides low impedance outputs which enable the analog signals to be accurately transmitted to the recording and analysis system.

The charge amplifier also has several different filter settings that are important to the integration process. It is necessary to highpass filter the input signal before the integration filter because any DC offset in the signal will cause the system to saturate. This is accomplished by an AC-coupling capacitor that immediately precedes the actual integrator circuit. Additional 2nd order Bessel highpass and lowpass filters are available with -3 dB corner frequencies that are selectable from 1 Hz to 1 KHz and from 100 Hz to 19.9 KHz respectively. These filters are used to bandlimit the signal to reduce noise that is inherently generated by equipment operating in the area of the test cell. 60 Hz noise and its harmonics are prevalent in unfiltered acceleration signals. It is impossible to discriminate between the actual acceleration signal and the noise; therefore, it is vital to use these filters to bandlimit the signal to the frequencies of the expected acceleration.

The integration circuit in charge amplifiers is constructed using op-amps and a feedback capacitor. The complete circuit is shown in figure 2-1. The s-domain transfer function of the complete integrating circuit was calculated to be: $H(s) = \frac{7200+1296s}{637000+217092s+131.8s^2}$. As the age of the charge amplifiers increase, the cost of repair and the percent error in the integration process continue to rise. The capacitance of the dielectric inside capacitors decreases with age, at an average logarithmic rate of 2.5% per decade hour [1]. This directly affects the accuracy of the integration curve over time and the cost of repairing or replacing these capacitors is high. The magnitude response of the analog integrator inside the charge amplifier and an ideal integration curve, which will be explained below, is compared in figure 2-2 and both the phase responses of the ideal and analog integrators are identical at -90 degree lag. The typical sampling rate when acquiring test data is 39,063 samples per second; therefore, all responses shown in this paper will

have the range of 0-19532 Hz, which is the Nyquist frequency. The analog integrator is well fitted as it is virtually identical to the ideal integrator but this is the absolute best response capable from analog components. The problem with the analog integrator, as mentioned above, is that the analog resistors and capacitors drift from their true value providing an incorrect integration curve. From testing several of the charge amplifiers, it was found that the aging components cause the magnitude response to be incorrect by 10-15% at any given frequency.

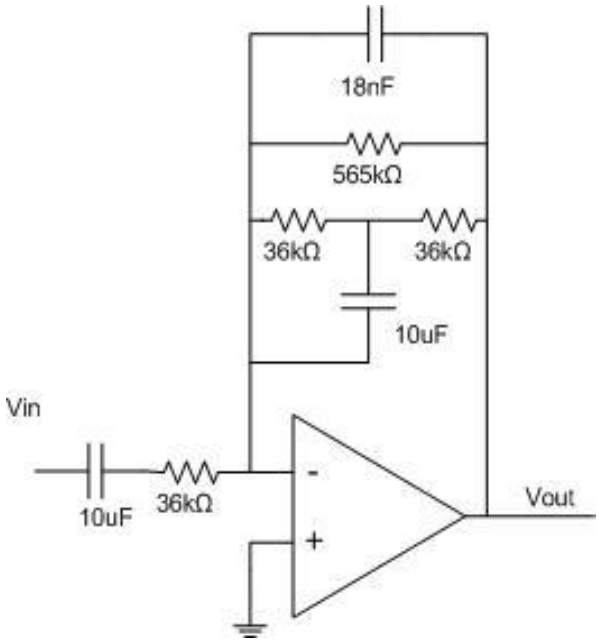

Figure 2-1: Integrating Circuit and DC Blocking Capacitor in Charge Amplifier

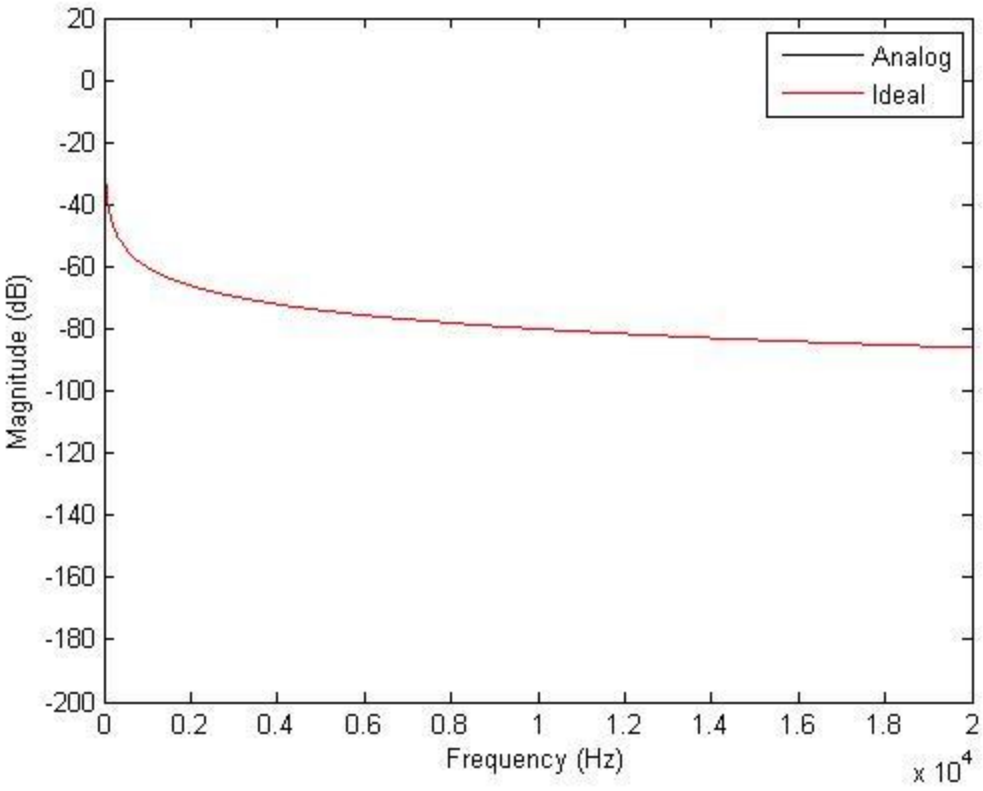

Figure 2-2: Analog Magnitude Response vs. Ideal Response

2.2 – Proposed Digital VMS

The previous section describes the shortcoming of the analog VMS system. The following dialogue will describe the advantages and improvements of changing to a digital VMS system. The charge signal from the accelerometer can be directly connected to a charge-to-voltage converter inside the test cell and an Analog-to-Digital device could then be placed inside the test cell or immediately outside. This would provide the preferred digital acceleration signal which could be processed by any digital filter that is desired. The hardware described above is available off the shelf for converting to a digital VMS. Although this thesis describes only the research and design of a digital integration filter needed to complete the digital VMS, it is also helpful to understand the entire VMS.

A digital signal, when compared to an analog signal, is less susceptible to the noise that plagues the test cell environment because a digital signal is simply a stream of 0's and 1's that is controlled by a voltage level that is on or off. If this is distorted by noise, it is inconsequential since a small amount of noise can be ignored when the signal reaches its destination and the data fidelity has not been compromised. For large amounts of noise, digital repeaters can be placed at certain points along the path to receive a noisy signal and retransmit the original signal. Due to the improved signal-to-noise ratio of digital signals over analog signals, the data signal fidelity would be improved. The data signals analyzed by the CADDMAS operator would be virtually noise free.

The digital acceleration data can be processed by digital integration filters to produce velocity and displacement data. Digital filters have accuracy characteristics not realizable by analog filters due to electrical component tolerances. Digital filters can also easily achieve practically any mathematical function or algorithm. With today's computer processing power it

is practical to develop digital filters of a much higher order than is feasible with analog filters. The higher order digital filters provide much sharper roll-offs and much better stop band attenuation than the current analog filters. Digital filters are also not subject to temperature drifts or aging electronics that plague their analog counterparts. All of these factors will improve the accuracy of a digital VMS when compared to the current analog VMS.

In addition to the accuracy issues, it would also be cheaper to switch to a digital VMS. Currently the charge amplifiers must be calibrated every three months at the Precision Measurement Equipment Laboratory (PMEL). During this process only the sensitivity of the acceleration input sensitivity is adjusted. The integrating filter response is not corrected. A digital system would not need to be calibrated at this regular interval so the cost savings of not calibrating 500 or more charge amplifiers would be substantial. The improvements in accuracy and cost savings would be considerable when converted to a digital VMS.

2.3 – Ideal Integration

The magnitude response of the analog filter is modeled from an ideal integration response. The mathematically correct solution, or ideal integrator, is used as the baseline for comparison purposes throughout this paper. Vibration is an oscillating, periodic motion therefore the mathematical solution is easy to illustrate. Take the simple sine wave: $x(t) = A*\sin(\omega*t)$, the mathematically correct integral is: $y(t) = (A/\omega)*\cos(\omega*t)$ plus a constant of integration. In summary, the ideal magnitude response, when ignoring the constant which must be removed and will be discussed later, is simply the magnitude of the original signal divided by the absolute value of the frequency while the phase of an ideal integrator is simply a 90 degree phase lag. The impulse response of the ideal digital integrator is:

$h(n) = 0.5 + \left(\frac{1}{\Pi}\right)\int_0^{\Pi n} \frac{sin(x)}{x}\, dx$ while the frequency response is known to be:

$H(\omega) = \Pi\delta(\omega) + \frac{1}{(j\omega)}$.

One way of comparison that will take both the magnitude and phase responses into consideration is to calculate the mean square error of the integrators. The mean square error is a statistical measure to calculate the amount by which an estimated value differs from the true value and is calculated using the formula: $MSE = \frac{1}{N}\sum_{i=1}^{N} |H\left(e^{j2\pi i/N}\right) - H'\left(e^{j2\pi i/N}\right)|^2$, where $H\left(e^{j2\pi i/N}\right)$ is each sample of the proposed integrator and $H'\left(e^{j2\pi i/N}\right)$ is each sample of the ideal integrator. By setting N=1000, each proposed integrator will be compared to the ideal integrator by taking 1000 samples from each and finding the average squared difference between the two. When compared to the ideal integration curve, the magnitude of the analog integrator mentioned above has a mean square error of 0.00002 which is an excellent comparison but as mentioned above it is not practical to expect in charge amplifiers that are over twenty years old.

An ideal filter has an infinitely long impulse response and extends all the way to negative infinity time. This also causes an ideal filter to be non-causal. Ideal filters have perfect attenuation but do not have to compensate for stop bands. Real-world signals from an accelerometer will not be infinitely long as is the case with an ideal signal; therefore, a practical digital filter needs to be designed that will minimize the error when compared to the ideal integrator that will allow the completion of the Digital VMS. The mean square error is one of the key relationships that will be used to determine each proposed integrator's validity and minimizing this value will be instrumental in developing a digital integrator that closely follows the ideal integrator.

2.4 – Previous Attempts

Previous efforts were made at AEDC to devise an integrator to fulfill such a purpose. Commonly known integrators such as the rectangle, trapezoidal, and Simpson's rules were first researched within known literature [2]. These methods are capable of providing accurate integrations but, as shown later in this paper; their limitations can be improved upon by various methods that will increase their accuracy substantially.

Other new methods not previously known were also investigated including taking the integral in its simplest form by calculating the Fast Fourier Transform (FFT) of the acceleration signal and simply dividing by its frequency [3]. Even though this method provides a correct answer, it is not fundamentally correct for if the inverse FFT were taken to return to the time domain the waveform would not have the correct phase lag. For the digital integrator to be essentially correct it must integrate in the time domain [4]. The rest of this document will detail the research and testing of a digital integrator to improve on these previous attempts so that a complete digital VMS can replace the analog VMS.

Chapter 3

Integration Filter Designs

When taking the integral of a mathematical equation, there are several different techniques that can be applied. Each will give a slightly different approximation to the actual solution and also have positives and negatives that must be weighed against each other. For this reason, eight different ways of integrating a digital signal were researched and compared to the ideal solution.

In the end the magnitude response will be the most important factor in determining which integration method is best for this application due to the engine manufacturers choice to view real time data in the frequency domain by having the CADDMAS take the FFT. This will ignore all errors created by the phase response by showing the true peak-to-peak value of the integral, which will be entirely composed by the magnitude response. Phase errors will only have relevance if the data is viewed in the time domain after the test is complete. These errors can be corrected for if the phase response is linear throughout the desired frequency range by simply advancing the signal in time by the amount of the phase lag. If the phase response of the integrator is non-linear, it cannot be corrected in the time domain. This issue can be helped by the fact that most usable data will be below 10 KHz because after integration anything above this level will too low to be meaningful. This will make integrators with correct phase lag in this range but incorrect phase lag above 10 KHz feasible for this application. Even though the magnitude response is more important than the frequency response, the phase response of the integrators cannot be ignored as it may be needed in post-test analysis of the data. The data

collected below will help in the choice of which integrator best follows the ideal integrator response and to be used in the digital VMS.

3.1 – Rectangle Rule

The rectangle rule, like many integrators, is an approximation to a definite integral made by finding the area of a series of rectangles. There are several different variations of the rectangular rule as the right corner, the mid-point, or the left corner of the rectangle can lie on the graph of the function with the bases of the rectangles running along the time axis with width Δt. The integral is approximated by summing the area of the rectangles within the limits of the definite integral. An illustration of this concept using the midpoint rule is shown in figure 3-1 but it is simple to see how the left or right corners, which are more common, could be used as well. The discrete sequence of the left corner integral can be written as: $y(n) = y(n-1) + x(n)\Delta t$. From this the frequency response yields: $H(e^{j\omega}) = \frac{\Delta t}{1-e^{-j\omega}}$. After taking the z-transform, the transfer function of the rectangular integrator is: $H(z) = \frac{\Delta t}{(1-z^{-1})}$. This is typically not a good approximation to the ideal integrator except at low frequencies where the denominator reduces to the desired magnitude.

With both the left and right corners the mean square error when compared to the ideal integrator is 0.2786. The comparison of the two magnitude responses along with the phase response of the rectangle rule integrator are shown in figure 3-2. While the phase of the rectangle rule is not correct when compared to the ideal integrator, it has a linear response throughout the frequency range so if needed it can be corrected during post-test data processing but would not be correct for real-time analysis of the signal. If the data were to be corrected post test, the mean square error reduced significantly to be 0.00024.

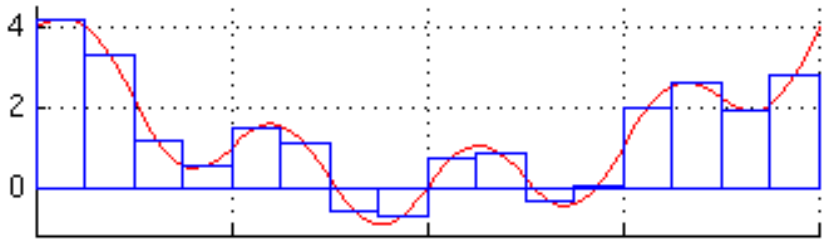

Figure 3-1: Rectangle Rule using the mid-point rule

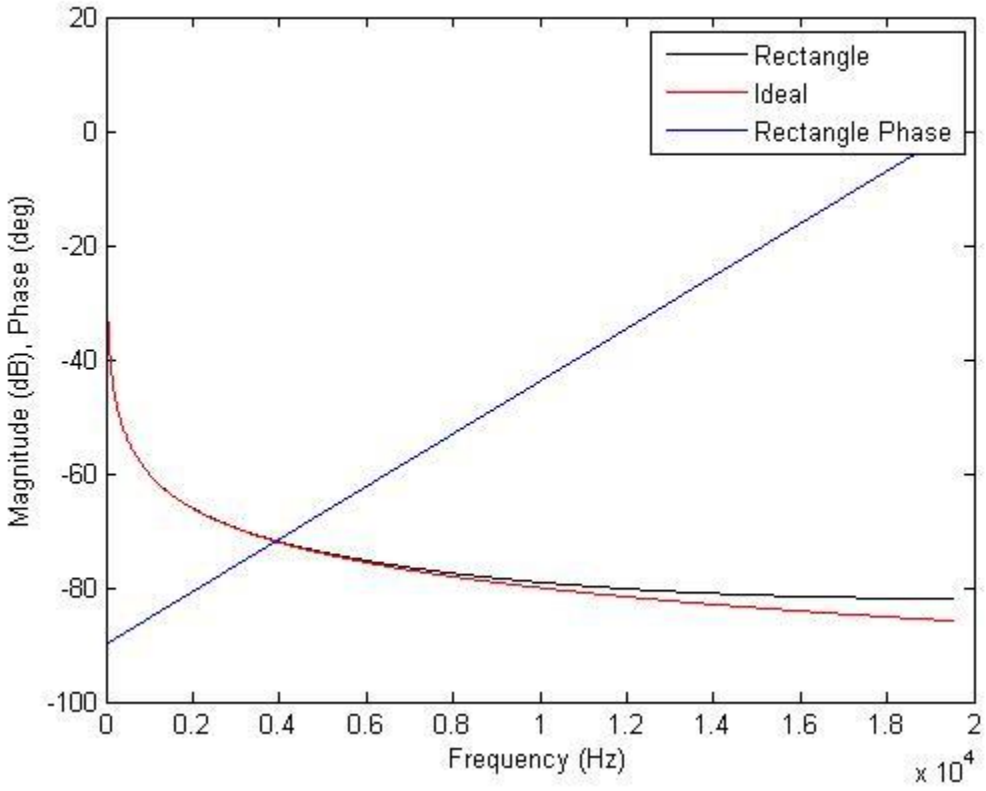

Figure 3-2: Magnitude and Phase Response of Rectangular Integration vs. Ideal Magnitude Response

3.2 – Trapezoidal Rule

Another common method for finding the approximate value of a definite integral is the trapezoidal rule. It is in a family of integrators called Newton-Cotes formulas that were developed by Isaac Newton and Roger Cotes. This group of formulas is based on evaluating the integrand at n+1 equally spaced points on the function. Newton-Cotes formulas of any degree can be constructed; however, the first and second degrees are more commonly used because the larger degrees have larger error.

Instead of using rectangles, trapezoids are summed to approximate the area underneath the curve. An illustration of this concept is shown in figure 3-3 over the same function as in figure 3-1. The trapezoidal rule is the first order Newton-Cotes formula. While the base of the trapezoid is still along the time axis, the top of the trapezoid is angled to conform more closely to the function as compared to the rectangle rule. The area of a single trapezoid can be calculated as: $A = (b-a) * \frac{\{f(a)+f(b)\}}{2}$. This gives us a closer approximation to the area underneath the curve of the function as compared to the rectangle rule.

The trapezoidal rule can be written in terms of a discrete sequence as:

$y(n) = y(n-1) + [x(n) + x(n-1)]\left(\frac{\Delta t}{2}\right)$. The frequency response of this equation is:

$H(e^{j\omega}) = \left(\frac{\Delta t}{2}\right)\frac{1+e^{-j\omega}}{1-e^{-j\omega}} = \left(\frac{\Delta t}{2}\right)\frac{\cos\left(\frac{\omega}{2}\right)}{j\sin\left(\frac{\omega}{2}\right)}$. As before with the rectangle integrator, this response is only accurate in the low frequency range with increasing inaccuracy as the frequency increases. Taking the z-transform, the transfer function can be arranged as: $H(z) = \Delta t\frac{(0.5+0.5z^{-1})}{(1-z^{-1})}$. When

compared to the ideal integrator, the trapezoidal rule has a mean square error of 0.0286. The phase response of the trapezoidal rule integrator along with the two magnitude responses are compared in figure 3-4. One advantage for the trapezoidal rule is that the phase response of the digital integrator follows the phase response of the ideal integrator exactly. This will minimize the phase error without any post-test processing but also this means that all of the error in this integrator comes from its magnitude response and it allows for real time analysis of the correctly integrated signals in the time domain.

3.3 – Simpson's Rule

The Simpson's rule or the second order Newton-Cotes integrator for approximating definite integrals was developed by Thomas Simpson (1710-1761) of Leicestershire, England. While the Simpson's rule is similar to both the rectangular and trapezoidal methods in that the base is along the time axis, it uses a quadratic polynomial to follow the function instead of straight line segments. An illustration of this is shown in figure 3-4 on the same function as the previous integrators. This results in better accuracy than the rectangular or trapezoidal methods when summing the area to approximate the integral. Simpson's rule can be derived by

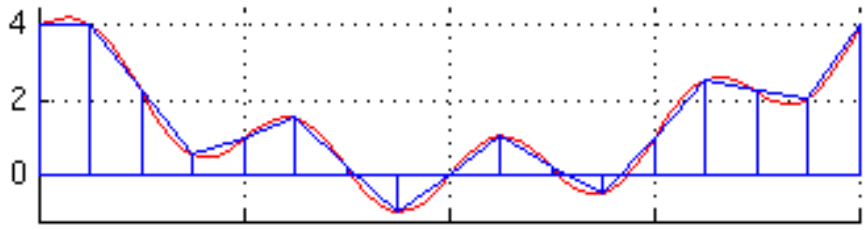

Figure 3-3: Integration using the Trapezoidal Rule

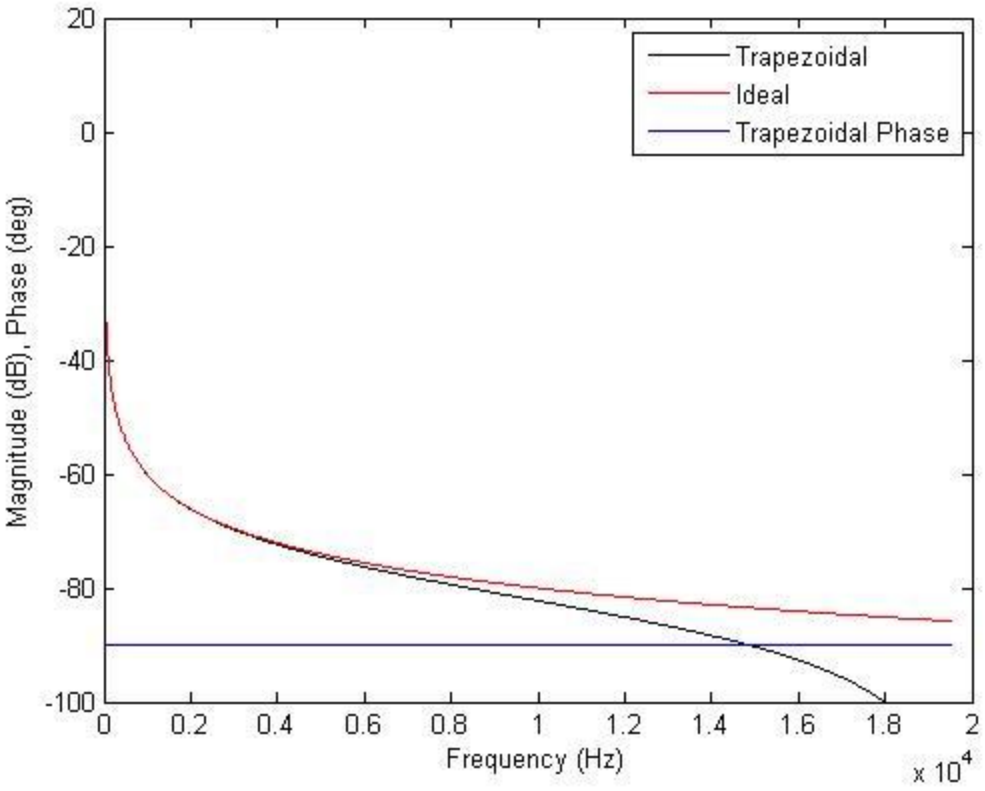

Figure 3-4: Magnitude and Phase Response of Trapezoidal Integration vs. Ideal Magnitude Response

integrating a third-order Lagrange Interpolating Polynomial fit to the function at three equally spaced points.

The area under the curve using Simpson's rule can be formulated as: $A = \frac{(b-a)\left\{f(a)+4f\left(\frac{a+b}{2}\right)+f(b)\right\}}{6}$. This can be written as a difference equation: $y(n) = y(n-2) + [x(n) + 4x(n-1) + x(n-2)]\left(\frac{\Delta t}{3}\right)$. The frequency response of this equation is: $H\left(e^{j\omega}\right) = \left(\frac{\Delta t}{3}\right)\frac{1+4e^{-j\omega}+e^{-2j\omega}}{1-e^{-2j\omega}} = \left(\frac{\Delta t}{3}\right)\frac{2+\cos(\omega)}{j\sin(\omega)}$. Taking the z-transform yields: $H(z) = \left(\frac{\Delta t}{3}\right)\frac{\left(1+4z^{-1}+z^{-2}\right)}{1-z^{-2}}$. While the Simpson's rule is again most accurate at low frequencies like the rectangular and trapezoidal methods, it has one disastrous property. At higher frequencies, especially near the Nyquist rate, the transfer function becomes unstable and approaches infinity. When compared to the ideal integrator, the Simpson's rule integrator has a mean square error of 5.32, which is due to its instability at higher frequencies. The phase response of the Simpson's integrator along with the two magnitude responses are compared in figure 3-6. The phase response of the Simpson's integrator matches the phase response of the ideal integrator exactly. Even with this advantage, the Simpson's integrator is unusable to many signal conditioning applications because even if there is a small amount of data at high frequencies the signal becomes unstable.

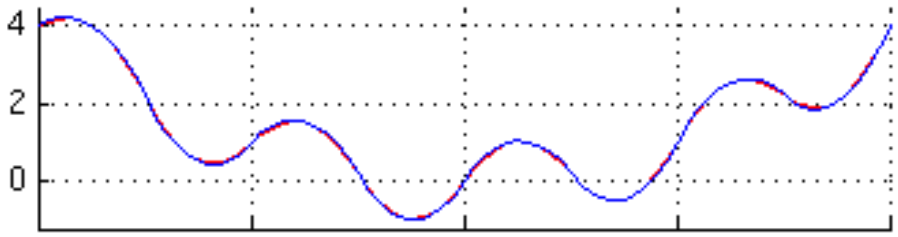

Figure 3-5: Integration using Simpson's Rule

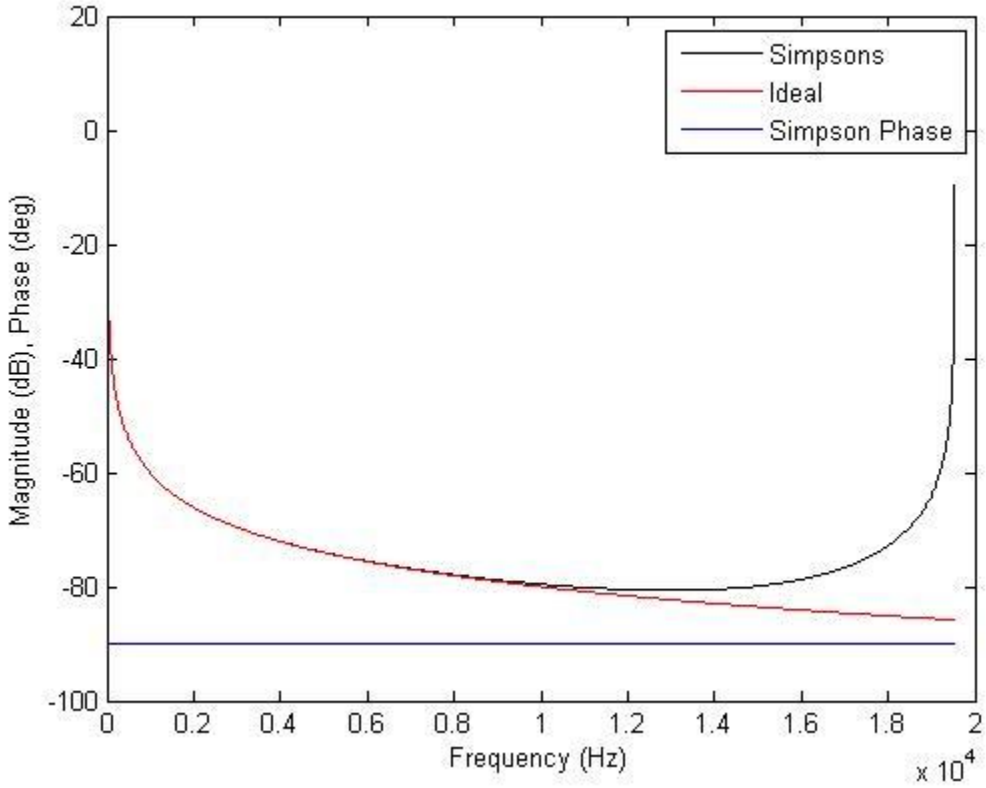

Figure 3-6: Magnitude and Phase Response of Simpson's Integration vs. Ideal Magnitude Response

3.4 – Bilinear Transform

The Bilinear Transform is a way of converting a continuous time transfer equation in the Laplace domain to its discrete time counterpart in the z-domain. It maps positions on the jω axis in the s-plane to the unit circle in the z-plane. The resulting digital filter will have the same characteristics of the original analog filter. This makes it possible to take the s-domain transfer equation from the charge amplifier integrating circuit which is: $H(s) = \frac{7200+1296s}{637000+217092s+131.8s^2}$, take the bilinear transform, and have a digital filter with the same magnitude and phase responses. Briefly, the Bilinear Transform is accomplished by taking the equation:

$s = \left(\frac{2}{\Delta t}\right)\frac{(1-z^{-1})}{(1+z^{-1})}$, where Δt is the sampling interval, and plugging it directly into the s-domain transfer function [2].

A common problem with taking the Bilinear Transform is distortion in the frequency axis because it maps the entire imaginary axis in the s-plane onto the unit circle in the z-plane. This can be compensated by pre-warping the cut-off frequencies before taking the Bilinear Transform. The pre-warped specifications can be used to create the desired digital system. An analog frequency is warped by taking the desired analog characteristic and mapping it to the z-plane by the following equation: $\Omega c = \left(\frac{2}{\Delta t}\right) tan\left(\frac{\omega_c}{2}\right)$ here Ω_c is the desired analog frequency and ω_c is the desired digital frequency. To prevent distortion along the axis while taking the bilinear transformation of the charge amp integrating circuit, the frequency needs to be pre-warped at 11 Hz. This will ensure that the gain and phase shift will be the same at 11 Hz on both the analog and digital filters.

Beginning with the transfer function of the integrating circuit, the digital transfer function

for this integrating filter using the method described above is: $H(z) = \Delta t \frac{190 + 0.0008z^{-1} - 190z^{-2}}{1 - 1.99z^{-1} + 0.99z^{-2}}$.

The frequency response of this integrator is: $H(e^{j\omega}) = \Delta t \frac{190 + 0.0008e^{-j\omega} - 190e^{-2j\omega}}{1 - 1.99e^{-j\omega} + 0.99e^{-2j\omega}}$. This integrator has a phase response that is a constant -90 degrees for all frequencies since the analog response was modeled after the trapezoidal rule. The mean square error of this integrator is 1.429 when compared to the ideal integrator, which is not as good as the digital trapezoidal integrator mentioned above even though the analog integrator was modeled after it and they share similar characteristics. The magnitude and phase responses from the bilinear integrator are compared to the magnitude response of the ideal integrator in figure 3-7.

3.5 – Simpson's Rule Delay Filter

The Simpson's Rule integrator is the most accurate integrator until it becomes unstable near the Nyquist frequency. In an attempt to minimize these flaws C.C. Tseng, a professor with Taiwan's National Kaohsiung First University of Science and Technology, suggests that the sampling period can be reduced from Δt to $\frac{\Delta t}{2}$ and a fractional delay filter cascaded with the original integrating filter [5]. This will allow for higher resolution and accuracy. The transfer function for this integrator can be simply obtained by the following equation:

$H(z) = \left(\frac{1}{2}\right) H_0(z^{-N})$, where N is the amount of delay. Delaying the filter 0.5 samples with a maximally flat group delay IIR all pass filter to approximate the fractional delay,

where $z^{1/2} \approx \frac{\left(\left(\frac{1}{3}\right) + z^{-1}\right)}{1 + \left(\frac{1}{3}\right)z^{-1}}$ resulted in the most success. This changes the z-transform of the

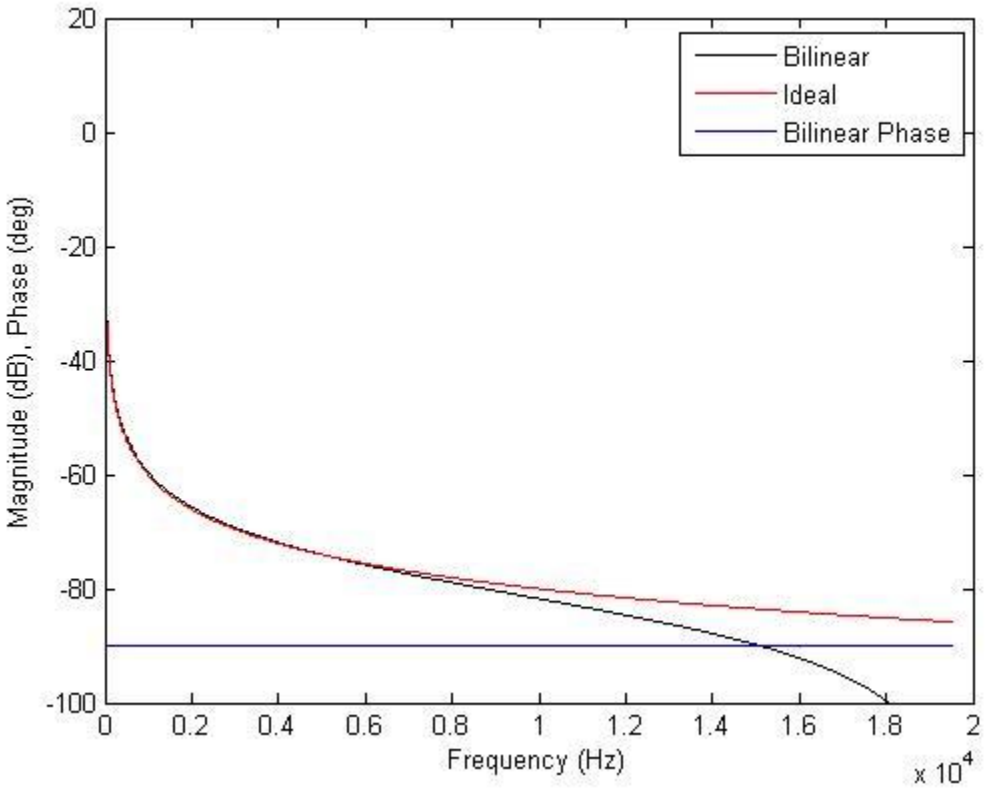

Figure 3-7: Magnitude Response and Phase Response of Bilinear Transform Integration vs. Ideal Magnitude Response

traditional Simpson's rule to be: $\boldsymbol{H(z) = \left(\frac{\Delta t}{6}\right)\frac{\left(1+4z^{-\frac{1}{2}}+z^{-1}\right)}{1-z^{-1}}}$. The combination of these equations results in the integrating transfer function: $\boldsymbol{H(z) = \left(\frac{\Delta t}{6}\right)\frac{7+16z^{-1}+z^{-2}}{3-2z^{-1}-z^{-2}}}$ **[5].**

The frequency response of this integrator is: $\left(e^{j\omega}\right) = \left(\frac{\Delta t}{3}\right)\frac{7+16e^{-j\omega}+e^{-2j\omega}}{3-2e^{-j\omega}-e^{-2j\omega}}$. If the frequency is very small this approximation yields the expression: $H\left(e^{j\omega}\right) \approx \frac{1}{j\omega}$ in the low frequency range, which is an exact approximation to the ideal integrator. It is shown in figure 3-8 that the error is smaller throughout the entire frequency band when compared to the original Simpson's integrator, especially in the higher frequency band where the Simpson's method becomes unstable. The mean square error when it is compared to the ideal integrator is 0.0371 which is excellent but it has one major drawback where the majority of the error in this integrator lies. The phase lag, also shown in figure 3-8, is non-linear to the point where the phase cannot be easily corrected for and will raise the overall error in the time domain anywhere above 5 KHz bandwidth. If this integrator were to be used in this frequency band only, the mean square error would be 0.0102.

3.6 – Weighted Least Squares Filter

There are several ways to create a digital filter if the desired magnitude response is known. One of these ways is the weighted least squares method. Least squares is commonly known as a way of fitting data points to a best fit quadratic line in statistical contexts. Instead of statistical data, we will be dealing with the magnitude response, or gain, of the filter. The least squares process defines the best fit line when the sum of the squared difference between axis values is at a minimum. Weighted Least Squares is a variant of the least squares method where

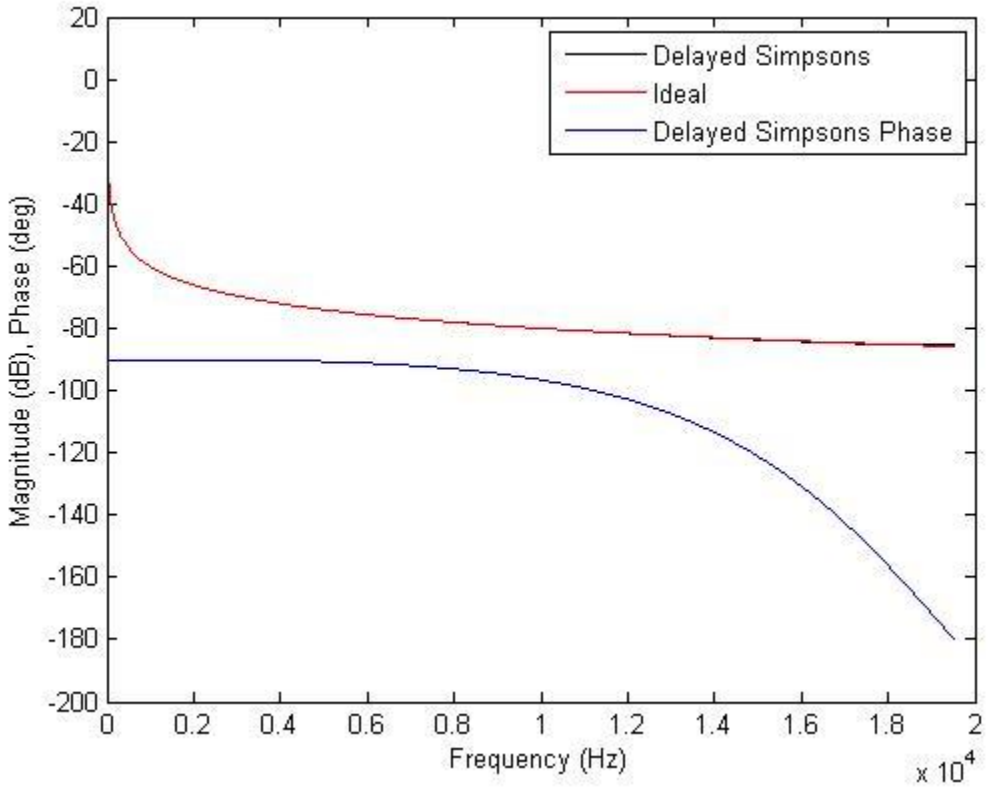

Figure 3-8: Magnitude and Phase Response of Delayed Simpson's Rule Integration vs. Ideal Magnitude Response

certain weights are put on areas of the data that is more important than other areas. Rik Pintelon and Johan Schoukens from Vrije University in Belgium states this is a capable way of constructing a digital integrating filter when the weights are spread equally throughout the frequency band [6].

The digital integrator using their method is formulated as follows. First, the digital filter is approximated using the Weighted Least Squares method. The resulting filters are unstable and must be stabilized by reflecting the unstable poles into the unit circle. This process does not change the magnitude response of the filter but it does alter the phase response. Further phase correction is needed in the form of an all-pass filter that will help linearize the phase [6].

Filters designed by the weighted least squares method are known to be more accurate on one end of the spectrum than the other end. It requires a fifth order equation to sufficiently approximate the ideal integrator in the frequency band up to 50% of the Nyquist frequency. The frequency response of this integrator is:

$H(e^{j\omega}) = \frac{1-8.42e^{-j\omega}+41.2e^{-2j\omega}-169.9e^{-3j\omega}+994.8e^{-4j\omega}+10183.3e^{-5j\omega}}{1-0.97e^{-j\omega}-0.02e^{-2j\omega}-0.01e^{-3j\omega}+0.0028e^{-4j\omega}-0.000267e^{-5j\omega}}$. The final z-domain transfer function for the integrator using the Weighted Least Squares design method is:

$H(z) = \frac{\left(1 - 8.42z^{-1} + 41.2z^{-2} - 169.9z^{-3} + 994.8z^{-4} + 10183.3z^{-5}\right)}{\left(1 - 0.97z^{-1} - 0.02z^{-2} - 0.01z^{-3} + 0.0028z^{-4} - 0.000267z^{-5}\right)}$. This transfer equation is quite a bit longer than others presented in this section and will require more computing resources.

When comparing this integrator to the ideal, the mean square error is 2951.6. This is largely due to the incorrect phase and the inaccuracy above 50% of the Nyquist rate. If the linear phase is corrected for post test the mean square error drops to 0.0009, which shows the amount

of fallacy in the phase response. The magnitude and phase responses are compared to the ideal magnitude response in figure 3-9.

3.7 – Modified Rectangle Rule Filter

From the frequency response and the impulse response of the ideal integrator it can be shown that $h(-n) = 1 - h(n)$ and $h(0) = \frac{1}{2}$. Using this information, a recursive association can be derived: $h(n) = h(n-1) + \left(\frac{1}{\Pi}\right)\int_{\Pi(n-1)}^{\Pi n} \frac{\sin(x)}{x}\, dx = h(n-1) + \frac{(-1)^{n-1}}{\Pi}\int_0^{\Pi} \frac{\sin(\varphi)}{\varphi+(n-1)\Pi}\, d\varphi$. Using this association along with: $h(0) = \frac{1}{2}$, the impulse response can be calculated numerically for $n > 0.5$ and the relation $h(-n) = 1 - h(n)$ can be used to find the values for $n < 0.5$ [7].

This can be used to modify the rectangle rule using the form: $H(z) = \Delta t \frac{z^{-1}}{(1-z^{-1})} + \frac{\alpha}{1+\beta z^{-1}}$. Setting $\alpha = 0.468$ and $\beta = 0.468$, which were found on a trial and error basis to minimize the mean square error, the following transfer function is calculated: $H(z) = \Delta t \frac{0.468+z^{-1}}{1-0.532z^{-1}-0.468z^{-2}}$. This results in a frequency response of: $H(e^{j\omega}) = \Delta t \frac{0.468+e^{-j\omega}}{1-0.532e^{-j\omega}-0.468e^{-2j\omega}}$. When comparing this integrator to the ideal integrator, the mean square error is 0.0468. This decreases the mean square error of the conventional rectangle integrator significantly; however, the phase response is not linear as before. This will not allow any improvement by post-test analysis. Both the magnitude and phase responses are shown in figure 3-10 along with the magnitude of the ideal integrator for comparison purposes.

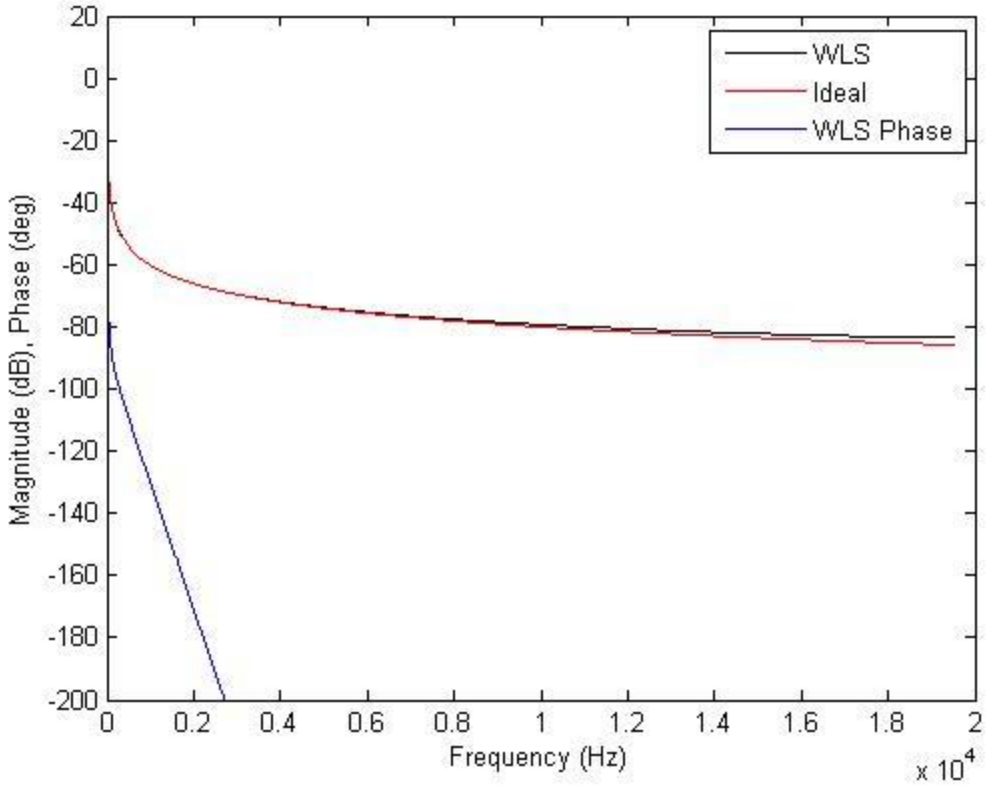

Figure 3-9: Magnitude and Phase Response of WLS Integrator vs. Ideal Magnitude Response

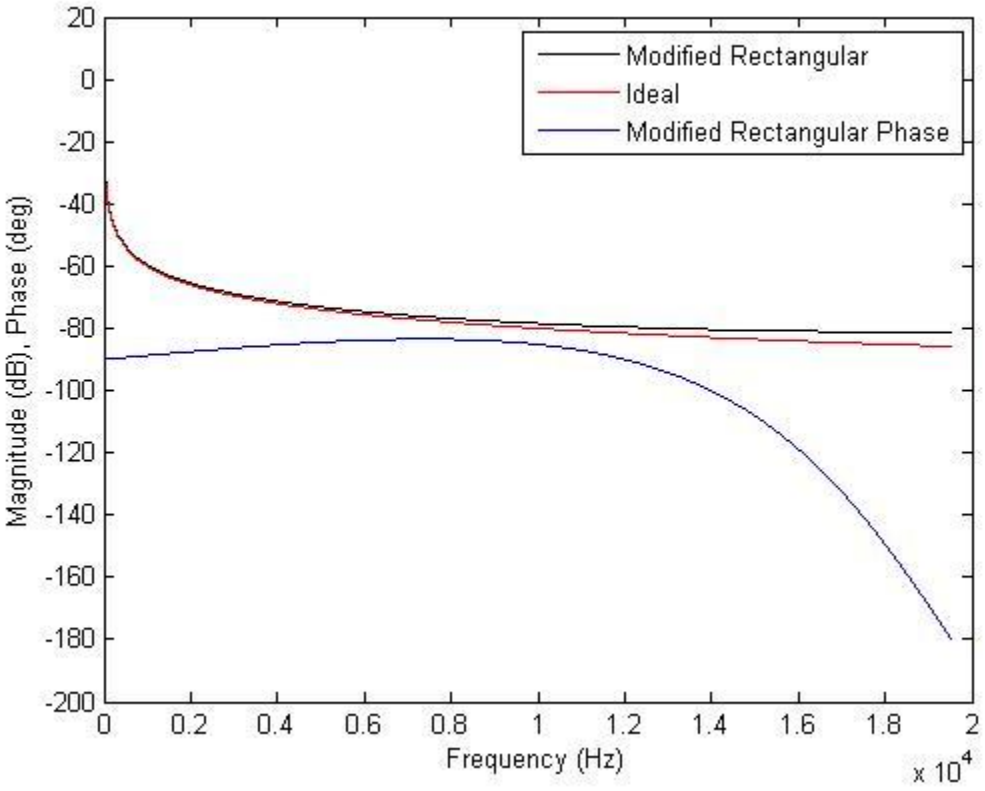

Figure 3-10: Magnitude and Phase Response of Modified Rectangle Rule vs. Ideal Magnitude Response

3.8 – Modified Trapezoidal Rule Filter

The process described above to modify the rectangle rule can be also applied to the trapezoidal rule. The most success was met by setting $\alpha = 0.078$ and $\beta = 0.74$, which were also determined by trial and error to minimize the mean square error, in the following equation: $H(z) = \Delta t \frac{0.5+0.5z^{-1}}{1-z^{-1}} + \frac{\alpha}{1+\beta z^{-1}}$. This leaves us with the following transfer function:

$H(z) = \Delta t \frac{0.5+0.945z^{-1}+0.289z^{-2}}{1-0.266z^{-1}-0.734z^{-2}}$. This function results in a frequency response of:

$H(e^{j\omega}) = \Delta t \frac{0.5+0.945e^{-j\omega}+0.289e^{-2j\omega}}{1-0.266e^{-j\omega}-0.734e^{-2j\omega}}$. The mean square error when comparing this integrator to the ideal integrator is 0.0152, which roughly cuts the error in the conventional trapezoidal rule in half. The magnitude and phase responses, along with the ideal magnitude response, are shown in figure 3-11. While the phase response is not exactly linear as it was before the modification, it is linear to approximately 12 KHz. This would encompass most usable data from an accelerometer and would only hinder viewing high frequency data, which is not necessary for this application.

3.9 – DC Blocking Filter

A DC-blocking filter is necessary before and after each integration step to ensure no DC offset is in the data signal. In addition to any DC offset that may be in the original acceleration signal, the constant of integration will add DC offset to the signal after each integration step. This must be removed before the next integration step or when the signal is integrated it will become unstable.

To remove DC offset from a signal in real-time, a single pole, single zero highpass IIR filter can be implemented. The filter is represented by the transfer function: $H(z) = \frac{1-z^{-1}}{1-a*z^{-1}}$. If $z = e^{j\pi F}$ is inserted into this function and the modulus is taken, the normalized magnitude and

phase transfer functions can be found. The magnitude response comes to:

$H(e^{j\omega}) = \frac{(1+a)\sin\left(\frac{\pi e^{j\omega}}{2}\right)}{\sqrt{1+a^2-2a\cos(\pi e^{j\omega})}}$ [7]. The single coefficient, a, can be found by setting the magnitude response of the filter to ½. This coefficient is used to determine the cut-on frequency of the filter and must vary between 0 and 1 for stability purposes. The equation to determine the pole is found to be: $a = \frac{\sqrt{3}-2\sin(\pi\omega)}{\sin(\pi\omega)+\sqrt{3}\cos(\pi\omega)}$, where ω is the cut-on frequency that is defined at the -6 dB point [7]. Setting F_c to 2 Hz, $a = 0.9994$ this allows for DC removal with minimum effect on the actual test data. This is shown in figure 3-12, which shows the magnitude and phase responses of the filter. At 10 Hz, which is the minimum frequency that actual data will reside, the magnitude of the DC-blocking filter is 0.95 and improves to 1.0 at approximately 14 Hz. The phase response of this filter also does not alter the data itself, as it is practically 0 after 10 Hz. This filter allows for successful DC removal while preserving data fidelity.

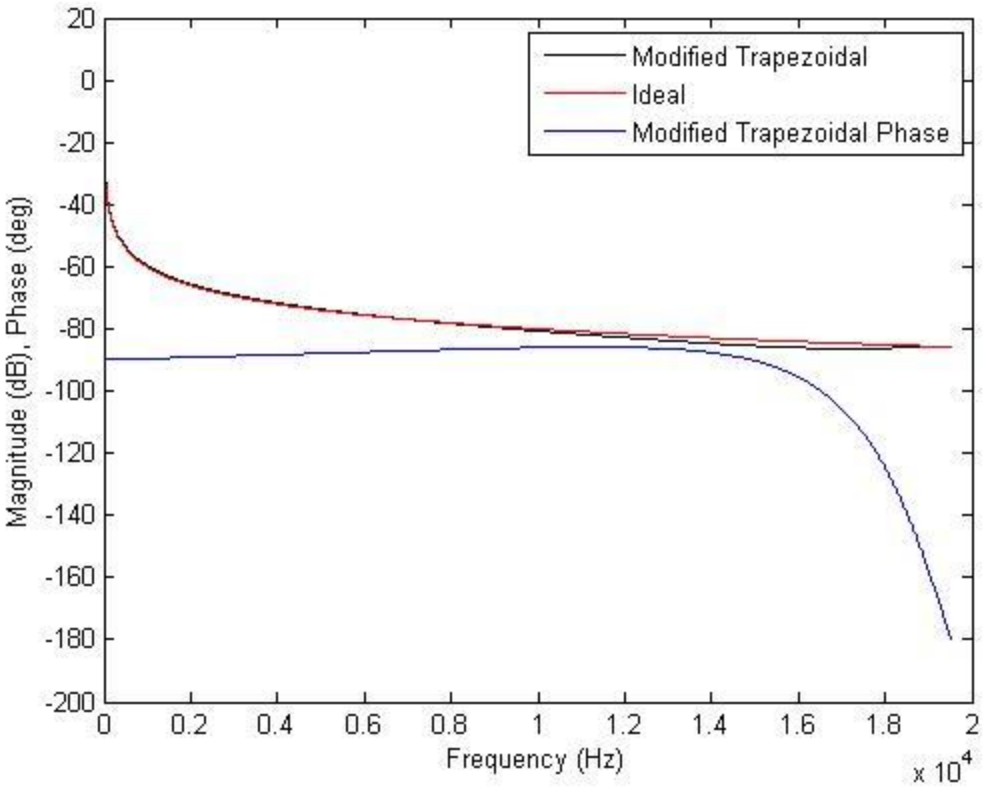

Figure 3-11: Magnitude and Phase Response of Modified Trapezoidal Rule vs. Ideal Magnitude Response

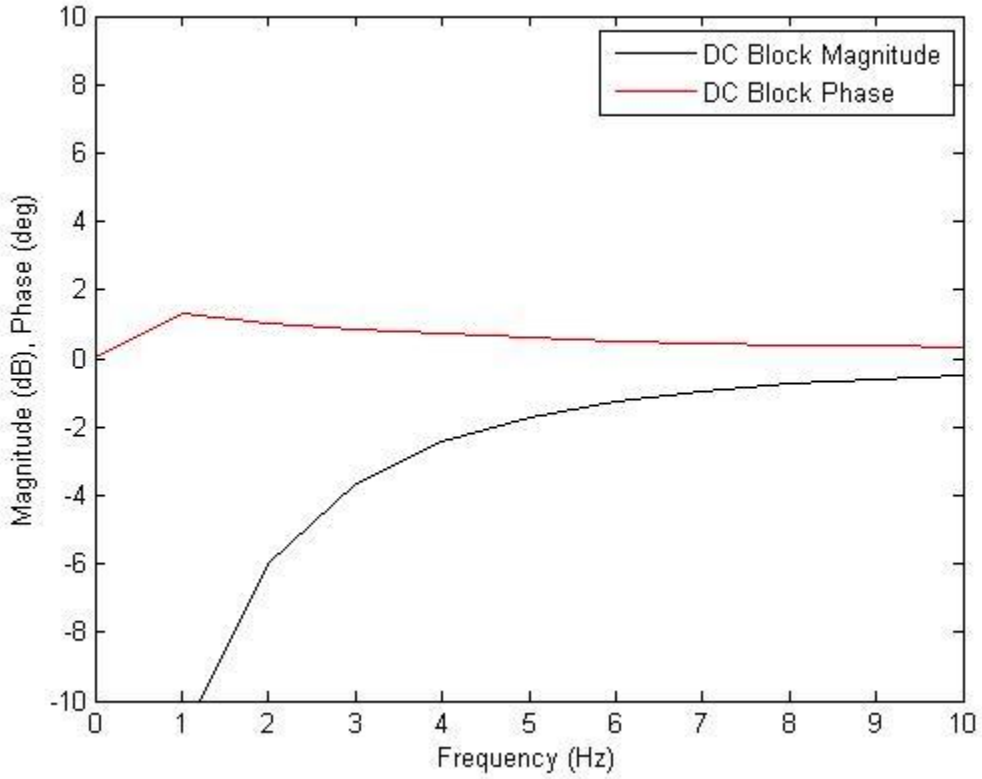

Figure 3-12: Magnitude and Phase Response of DC Blocking Filter

Chapter 4

Integration Test Results

After the eight candidate integrating filters were researched, a method for comparing them with real data was needed. Data was acquired for this purpose from two different sources. The first data set was acquired directly from an accelerometer during a test in a turbine engine facility at AEDC. Additionally, the velocity and displacement data from the analog integrating charge amplifier was recorded for comparison to the digital integrating filters. The acceleration data was imported into MATLAB via a comma separated file from CADDMAS. MATLAB is a mathematics program that was used to run the acquired data through each candidate digital filter and process the results. The next set of data was acquired using a simulated signal generated by MATLAB at 600 Hz, 3000 Hz, 6000 Hz and 10000 Hz. These frequency values were chosen to show values across the entire frequency spectrum to get a broader look at each integrator even though no usable data is present during testing.

First, the acceleration data was sent through the DC Blocking filter to remove any native DC bias in the recorded signal. After this, the remaining sinusoidal signal was passed through each integrating filter to find the corresponding velocity value. After taking the FFT to change to the frequency domain, the true peak-to-peak values of the nominal vibration frequency are shown. The velocity value was then compared to the mathematical solution, which was found by dividing the magnitude of the acceleration signal by the frequency, to find a relative percent error of each digital integrator's velocity value at the single peak frequency. The velocity time signal

was then passed through the DC Blocking filter and the same integrating filter again to find the corresponding displacement value. The FFT was taken and the value compared to the mathematically correct displacement value to find the relative percent error of each integrator's displacement value. This process was completed for each of the eight integrating filters described in the preceding section.

While the mean square error of each integrator is over the entire frequency band, the data below is centered at 1644 Hz because that is where the meaningful test data will be centered. This means that the mean square error may not give a good indication of the accuracy of the integrators at a single frequency since it is an average. Given that the data is viewed after taking the FFT, all errors in the phase domain will be ignored since only the data magnitude is being viewed but this is also the way the data is observed real time during the test so this is the exact same process as would happen during an actual test.

The original acceleration signal has been passed through the low-pass filter of the charge amplifier and is shown in figure 4-1. The peak-to-peak value is 17.42 G's at 1644 Hz. The mathematically correct solution for this integral is 0.651 inches/second peak-to-peak for velocity and 0.06303 mills peak-to-peak for displacement. The results of the analog integrator are shown below in figure 4-2 for velocity and figure 4-3 for displacement. The error shown by the analog integrator is substantially improved by the use of the digital integrators researched in this paper. The results for all filters using the same acceleration signal are shown below in figures 4-4 through 4-19 and summarized in table 4-1. The results for the simulated signals are shown in tables 4-2 through 4-5.

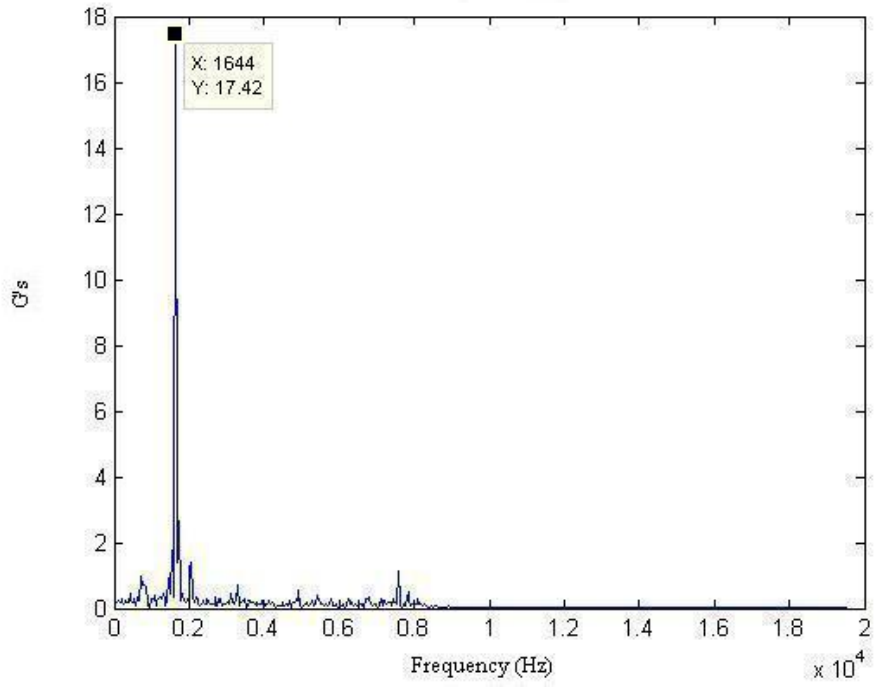

Figure 4-1: Magnitude Spectrum of the Input Acceleration Signal Acquired from Turbine Engine Test

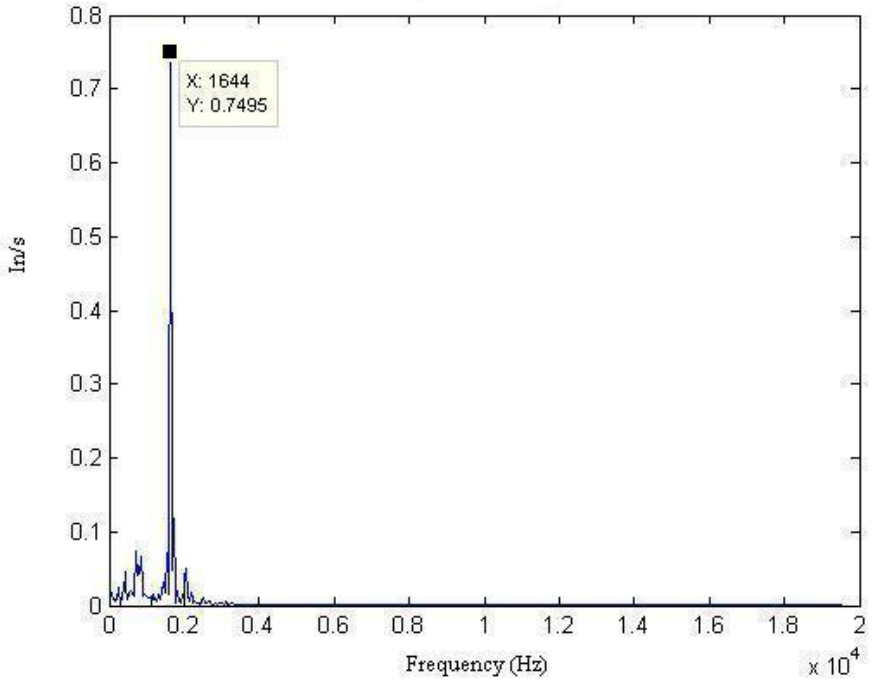

Figure 4-2: Magnitude Spectrum of Velocity Signal from Analog Integrating Charge Amplifier

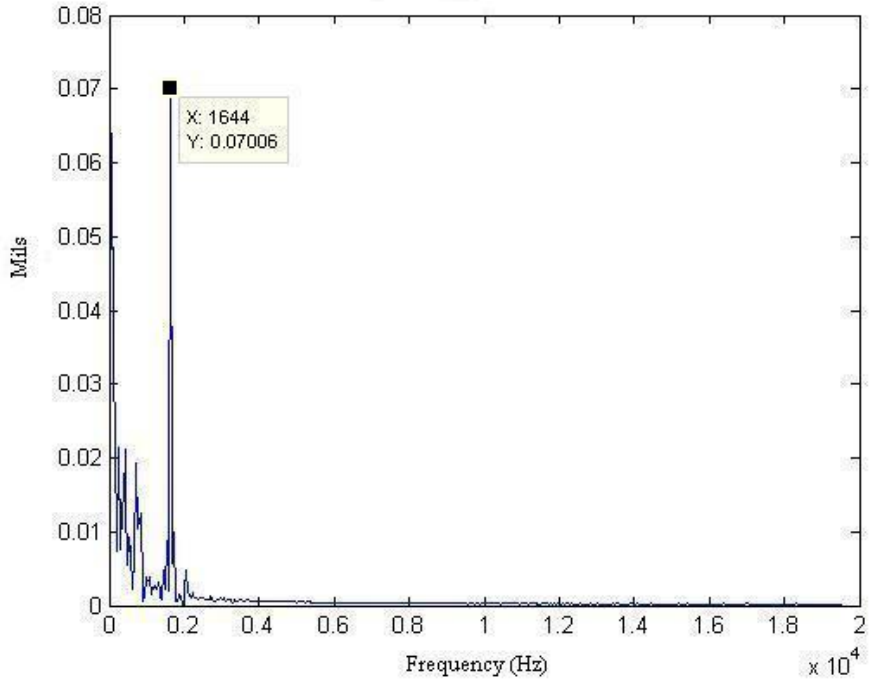

Figure 4-3: Magnitude Spectrum of Displacement Signal from Analog Integration Charge Amplifier

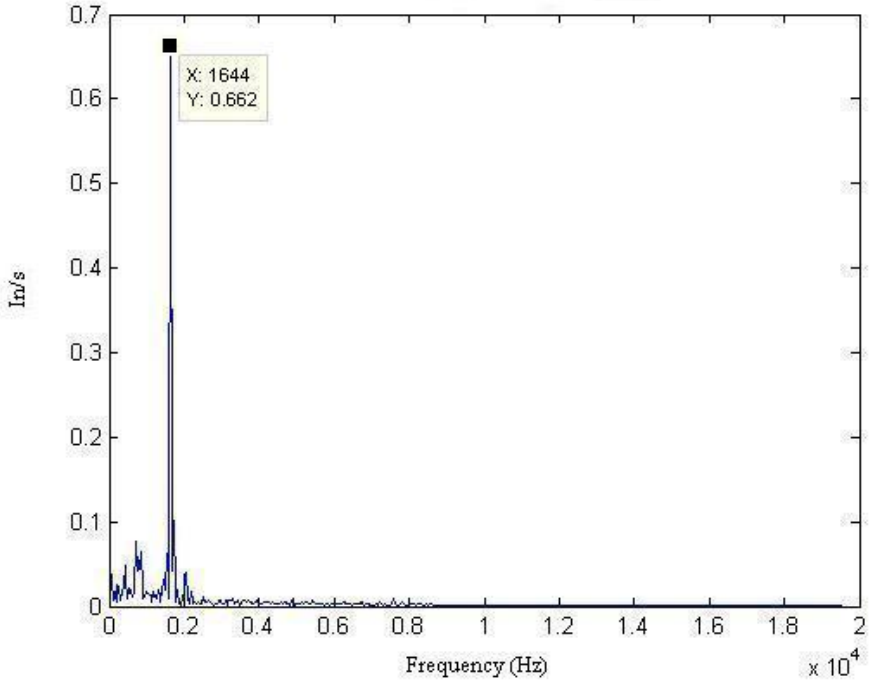

Figure 4-4: Magnitude Spectrum of Velocity Signal from Digital Rectangle Rule

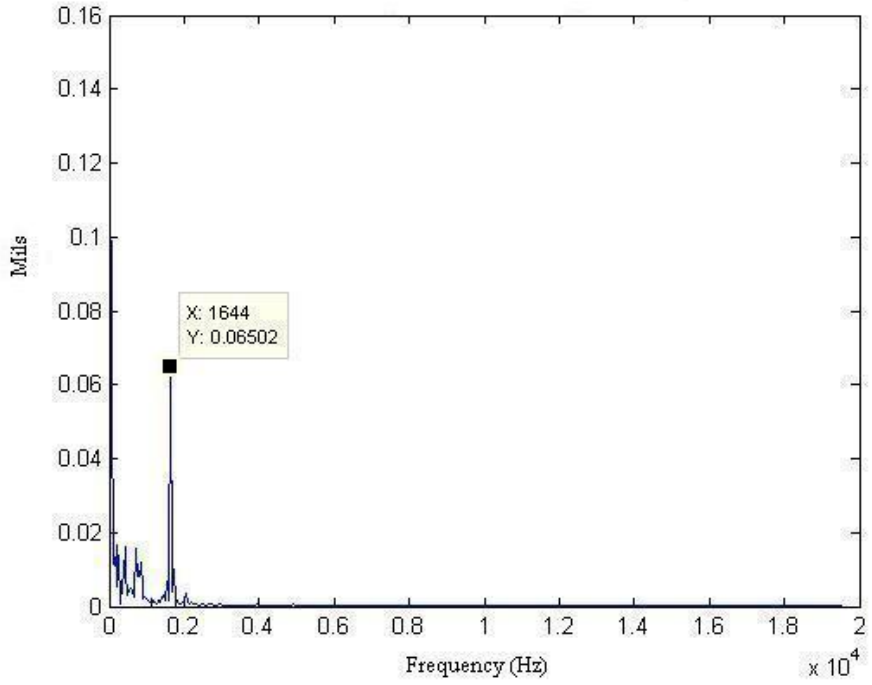

Figure 4-5: Magnitude Spectrum of Displacement Signal from Digital Rectangle Rule

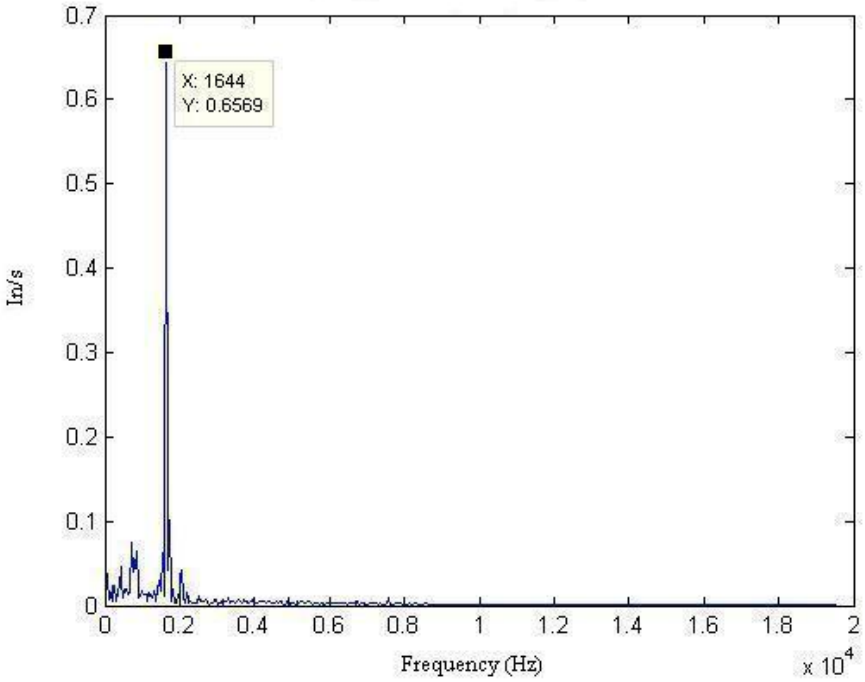

Figure 4-6: Magnitude Spectrum of Velocity Signal from Digital Trapezoidal Rule

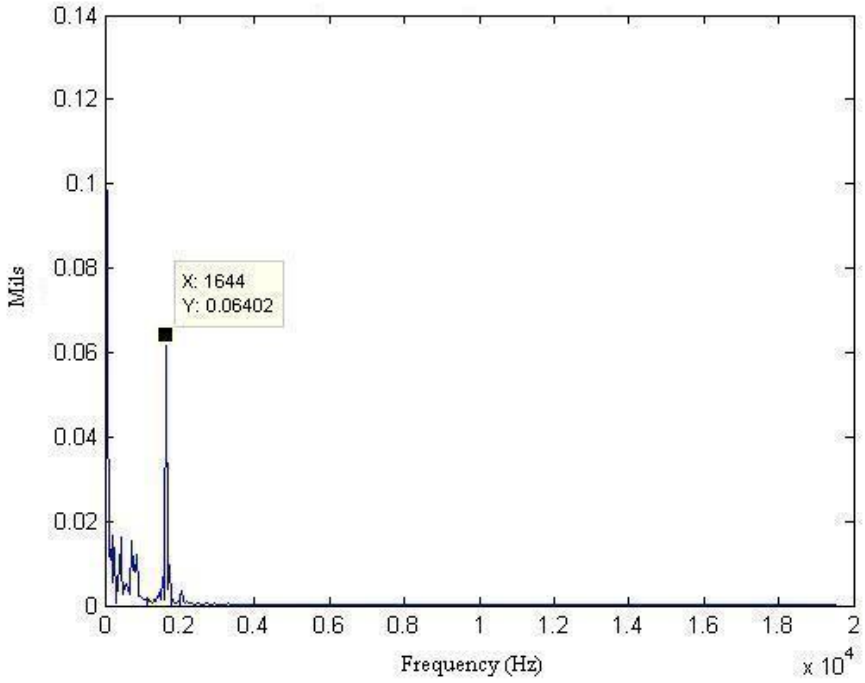

Figure 4-7: Magnitude Spectrum of Displacement from Digital Trapezoidal Rule

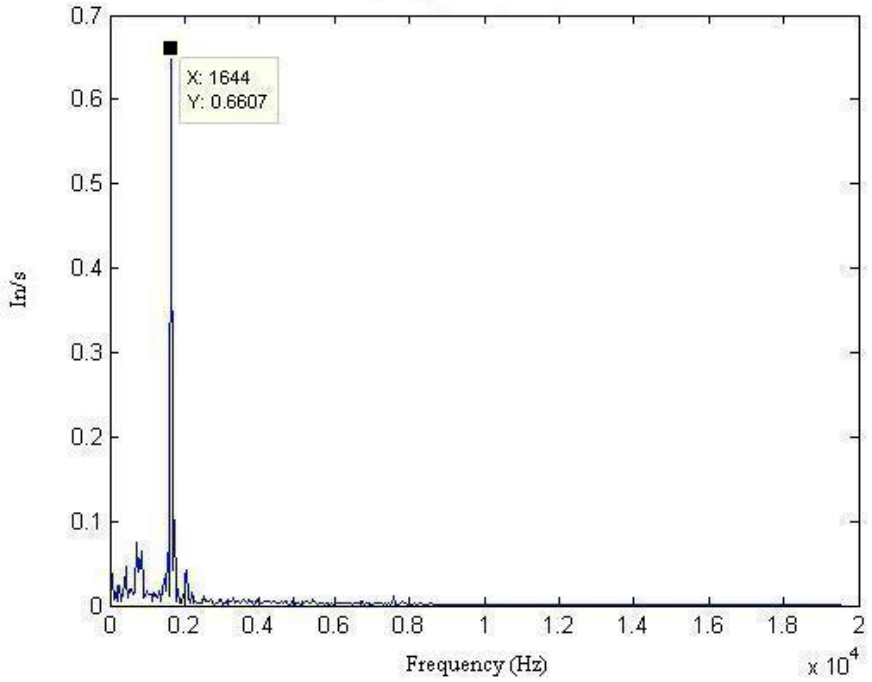

Figure 4-8: Magnitude Spectrum of Velocity Signal from Digital Simpson's Rule

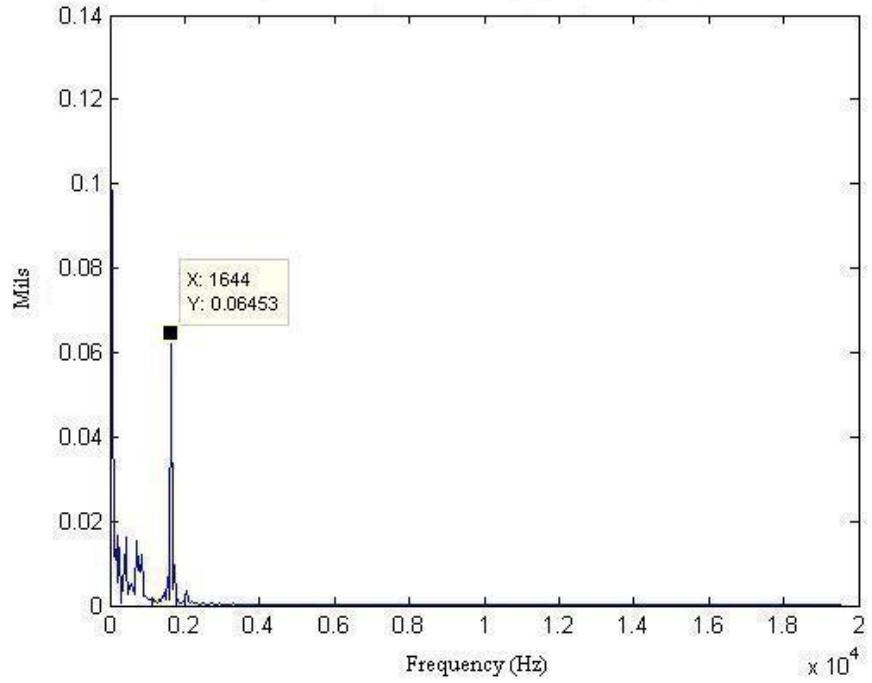

Figure 4-9: Magnitude Spectrum of Displacement Signal from Digital Simpson's Rule

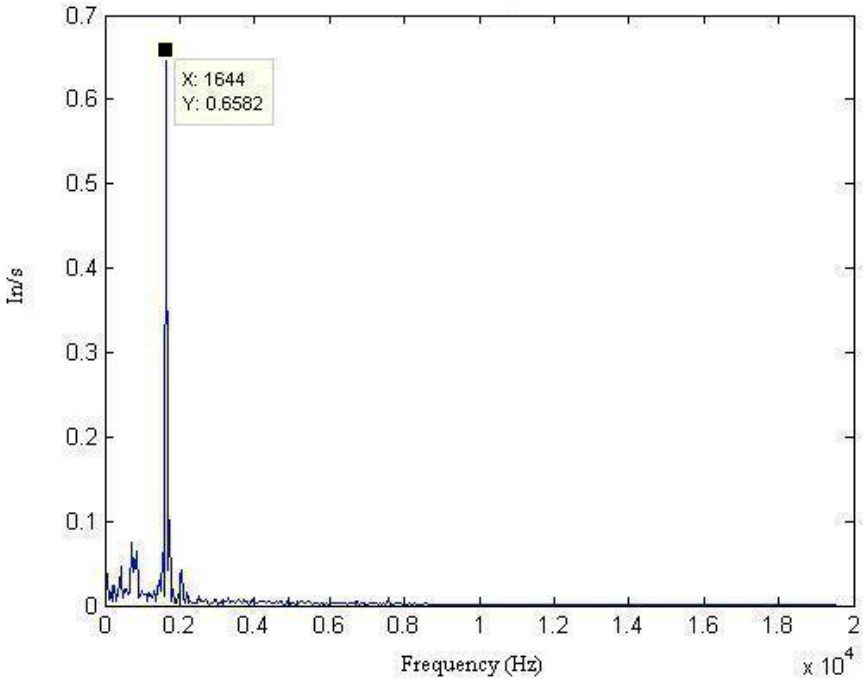

Figure 4-10: Magnitude Spectrum of Velocity Signal from Bilinear Transform Integrator

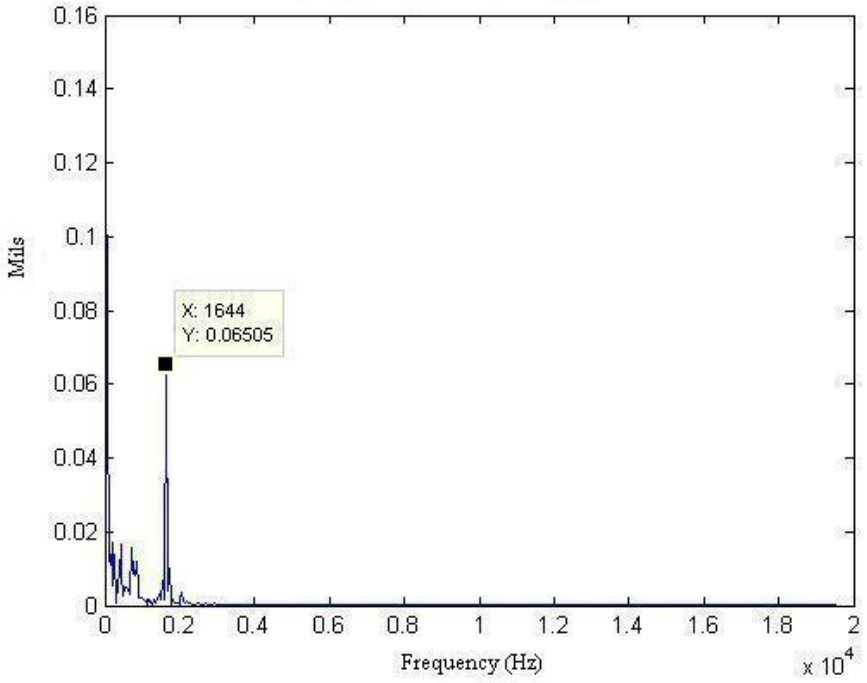

Figure 4-11: Magnitude Spectrum of Displacement from Bilinear Transform Integrator

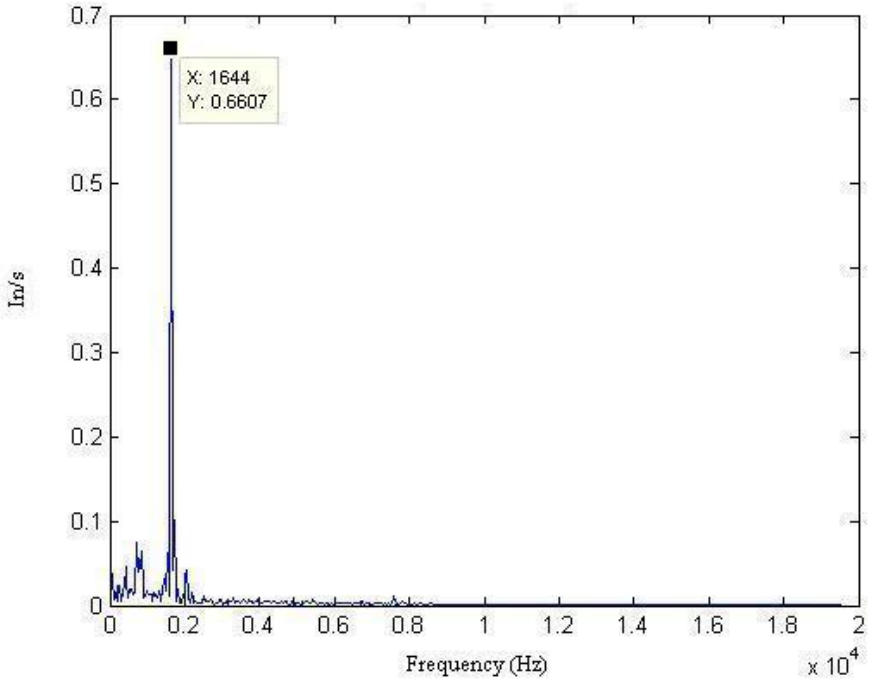

Figure 4-12: Magnitude Spectrum of Velocity from Digital Delayed Simpson's Rule

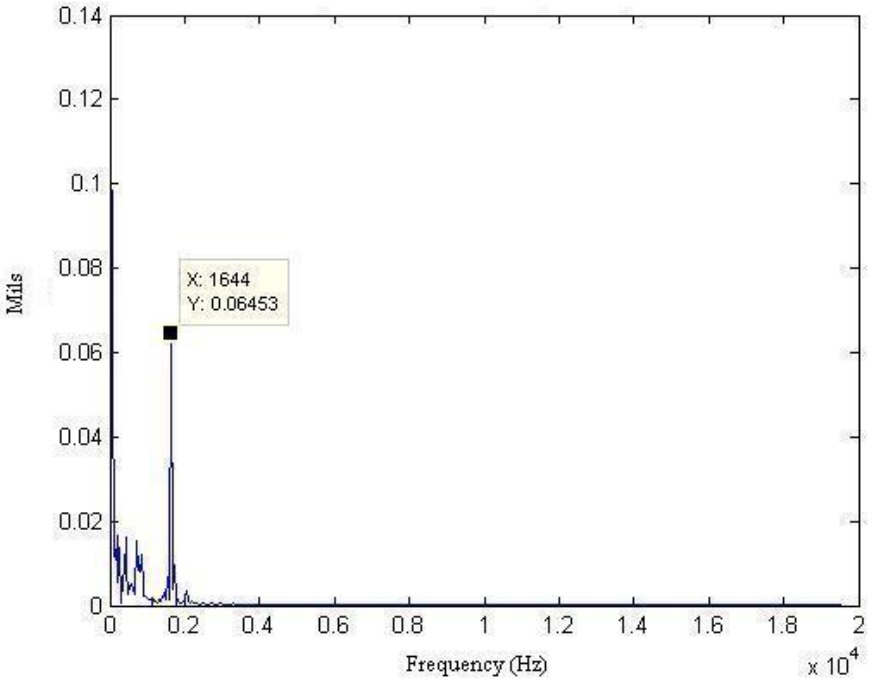

Figure 4-13: Magnitude Spectrum of Displacement from Digital Delayed Simpson's Rule

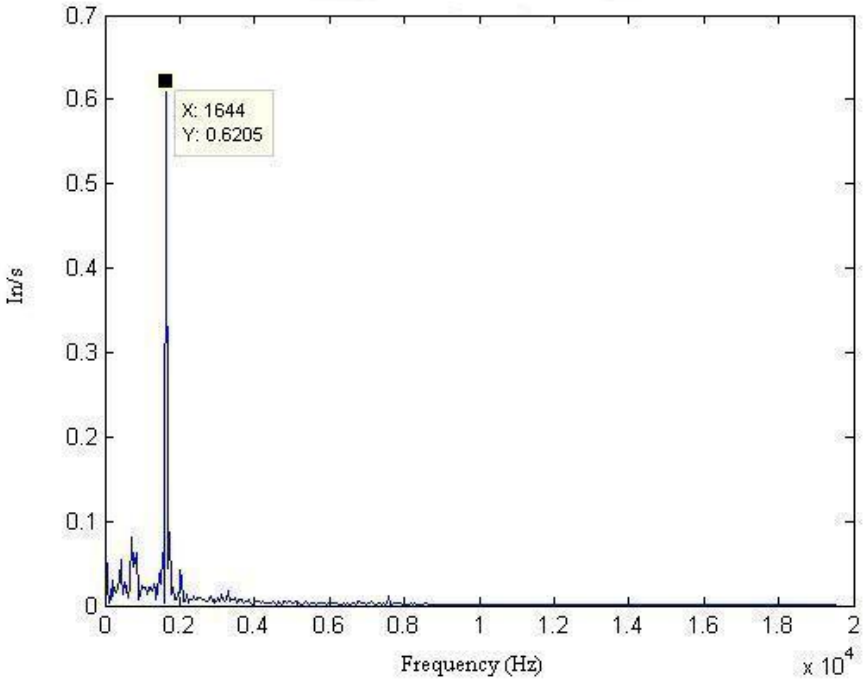

Figure 4-14: Magnitude Spectrum of Velocity Signal from WLS Integrator

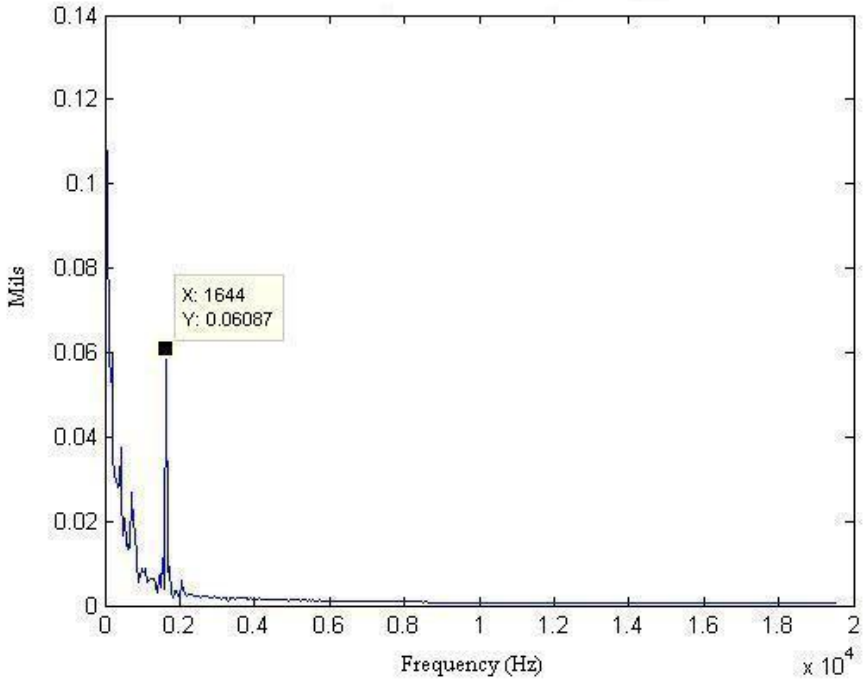

Figure 4-15: Magnitude Spectrum of Displacement from WLS Integrator

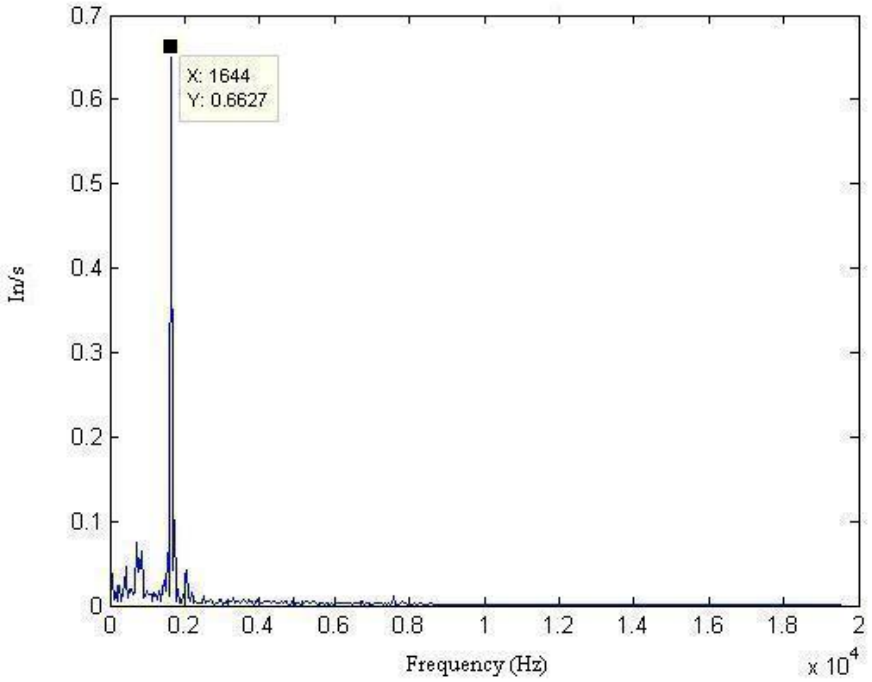

Figure 4-16: Magnitude Spectrum of Velocity from Digital Modified Rectangle Rule

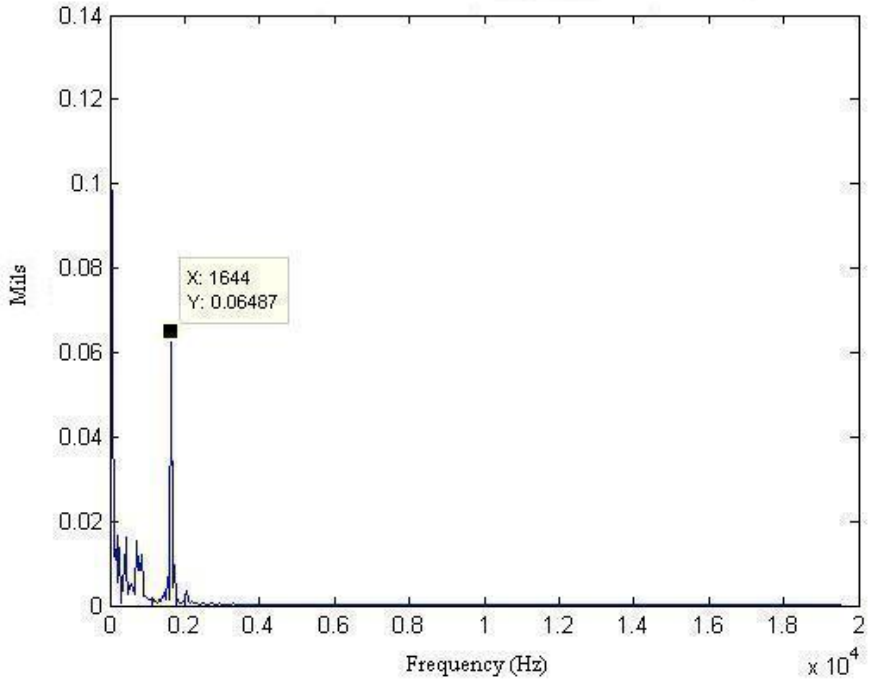

Figure 4-17: Magnitude Spectrum of Displacement from Digital Modified Rectangle Rule

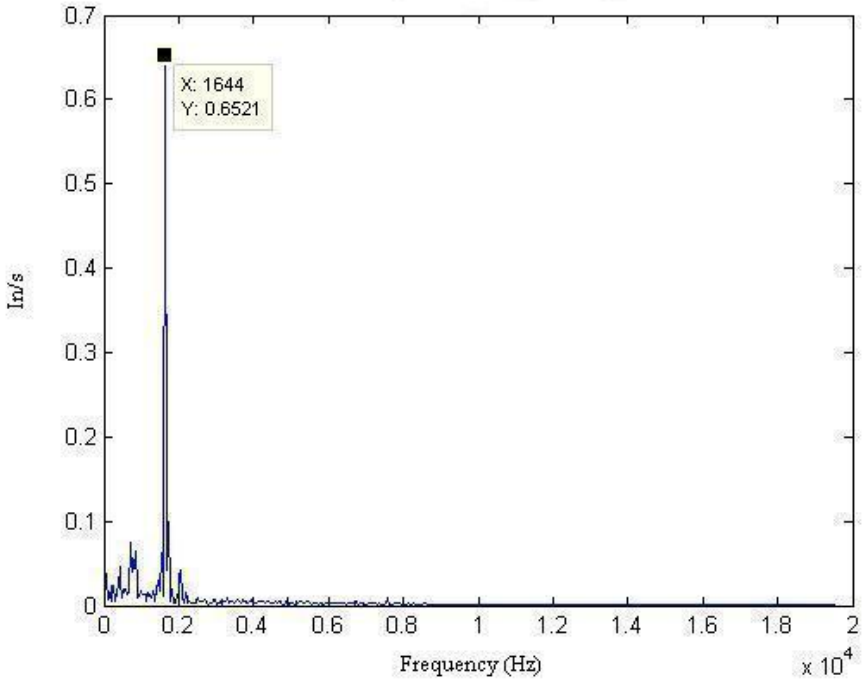

Figure 4-18: Magnitude Spectrum of Velocity Signal from Digital Modified Trapezoidal Rule

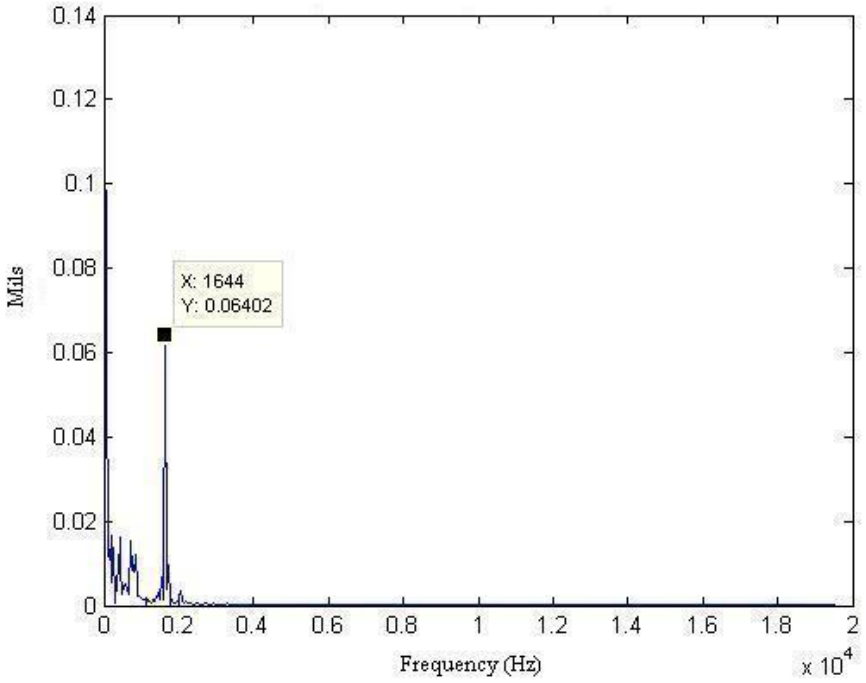

Figure 4-19: Magnitude Spectrum of Displacement from Digital Modified Trapezoidal Rule

Table 4-1: Summarized Results of Integrators from Test Data

Integrator:	MSE:	% Error Velocity:	% Error Displacement:
Analog	0.00002	15.1%	11.7%
Rectangle Rule	0.2786	1.7%	3.1%
Trapezoidal Rule	0.0286	0.9%	1.5%
Simpson's Rule	5.32	1.4%	2.3%
Bilinear	1.429	1.1%	3.2%
Delayed Simpson's	0.0371	1.4%	2.3%
WLS	2951.6	4.6%	3.4%
Modified Rectangle	0.0468	1.7%	2.9%
Modified Trapezoidal	0.0152	0.16%	1.2%

Table 4-2: Summarized Results of Integrators at 600 Hz

Integrator:	MSE:	% Error Velocity:	% Error Displacement:
Rectangle Rule	0.2786	-1.48%	5.88%
Trapezoidal Rule	0.0286	-2.52%	3.76%
Simpson's Rule	5.32	-1.47%	6.0%
Bilinear	1.429	-2.95%	2.82%
Delayed Simpson's	0.0371	-4.95%	-1.31%
WLS	2951.6	-2.17%	4.49%
Modified Rectangle	0.0468	-2.52%	3.76%
Modified Trapezoidal	0.0152	-2.45%	3.88%

Table 4-3: Summarized Results of Integrators at 3000 Hz

Integrator:	MSE:	% Error Velocity:	% Error Displacement:
Rectangle Rule	0.2786	-1.63%	5.68%
Trapezoidal Rule	0.0286	-3.34%	2.05%
Simpson's Rule	5.32	-2.96%	2.88%
Bilinear	1.429	-3.34%	2.13%
Delayed Simpson's	0.0371	-2.21%	4.47%
WLS	2951.6	-4.16%	0.31%
Modified Rectangle	0.0468	-1.63%	5.68%
Modified Trapezoidal	0.0152	-1.70%	5.48%

Table 4-4: Summarized Results of Integrators at 6000 Hz

Integrator:	MSE:	% Error Velocity:	% Error Displacement:
Rectangle Rule	0.2786	-9.21%	-10.06%
Trapezoidal Rule	0.0286	1.31%	12.14%
Simpson's Rule	5.32	-9.19%	-9.93%
Bilinear	1.429	-2.46%	3.95%
Delayed Simpson's	0.0371	-1.73%	0.19%
WLS	2951.6	-2.17%	4.54%
Modified Rectangle	0.0468	1.13%	12.14%
Modified Trapezoidal	0.0152	0.6%	10.56%

Table 4-5: Summarized Results of Integrators at 10000 Hz

Integrator:	MSE:	% Error Velocity:	% Error Displacement:
Rectangle Rule	0.2786	8.76%	29.12%
Trapezoidal Rule	0.0286	-23.65%	-36.37%
Simpson's Rule	5.32	2.16%	13.9%
Bilinear	1.429	-23.67%	-36.17%
Delayed Simpson's	0.0371	-2.19%	4.44%
WLS	2951.6	3.69%	17.34%
Modified Rectangle	0.0468	8.77%	29.12%
Modified Trapezoidal	0.0152	5.74%	22.02%

Chapter 5

Summary and Recommendations

This thesis has presented a description and shortcomings of the current analog VMS. It was then shown how a digital VMS can improve these shortcomings. With hardware available, only a digital integration filter was needed to complete the digital VMS. Eight candidate digital integrators were proposed. Each would substantially improve the accuracy, reduce calibration costs, and eliminate current noise problems that plague the analog integrator. A detailed description of each digital integrating filter was then given. Each filter was then evaluated with simulated signals and real test data to show the actual results that would be provided real-time to the test customers. This proved that a digital VMS would significantly improve the accuracy of the test data. Finally, one digital integrator will be chosen below for recommendation to complete the digital VMS.

Each of the eight digital integrators shown above would improve upon the analog integrator currently in use but one must be chosen to complete the digital VMS. The Simpson's Rule filter, due to its instability at high frequency, and the Weighted Least Squares filter, given its poor phase accuracy, should be immediately eliminated. The Rectangle, Modified Rectangle, Trapezoidal and Bilinear filters are capable filters that would give satisfactory results in the VMS but the Delayed Simpson's and Modified Trapezoidal Rule give the superior results from this study. Both these integrators have advantages over the others given their low mean square error and excellent outcome with test data. If the phase needs to be absolutely correct or the data is

high frequency then the Delayed Simpson's Rule should be used. If phase is not as important and the data is in the lower section of the frequency band then the Modified Trapezoidal can be used since it shows slightly better accuracy. If one overall filter needs to be used the author of this thesis would recommend that the Delayed Simpson's Rule be used due to it having the best results over the entire frequency band while the phase response is correct at the lower frequency range where most of the usable data is located.

References

References

1. Johanson Dielectrics Inc. Ceramic Capacitor Aging Made Simple. Sylmar, CA: Christopher England. 2006.
2. Oppenheim, Alan V. & Schafer, Ronald W. Digital Signal Processing. Englewood Cliffs, New Jersey: Prentice-Hall, Inc. 1975.
3. Phil Voyles, personal communication
4. Brandon Jones, personal communication
5. C.C. Tseng. Digital Integrator Design Using Simpsons Rule and Fractional Delay Filter. IEEE Proc.-Vis. Image Signal Process., Vol. 153, No. 1. 2006. 79-85.
6. Pentelon, Rik & Shoukens, Johan. Real Time Differentiation and Integration by Means of Digital Filtering. IEEE Transactions on Instrumentation and Measurement. Vol. 39. No. 6. 1990. 923-927
7. L. Montgomery Smith, personal communication
8. de Freitas, J.M. The DC Blocking Filter. 2007. http://www.mathworks.com/matlabcentral/fileexchange/loadFile.do?objectId=13792&objectType=file.

VITA

Charles Matthew Rose was born on August 4, 1982 in Winchester, Tennessee. He grew up in Winchester and graduated from Franklin County High School in 2000. Matt attended the University of Tennessee-Knoxville and received a Bachelors of Science degree in Electrical Engineering in 2004. Following graduation, Matt accepted an engineering position in the Information Technology department at AEDC. He also continued his education at the University of Tennessee Space Institute and received his Masters of Science degree in Electrical Engineering in May of 2009.